The haplo-diplontic life cycle expands niche space of coccolithophores

Joost de Vries[1, 2], Fanny Monteiro[1], Glen Wheeler[2], Alex Poulton[3], Jelena Godrijan[4], Federica Cerino[5], Elisa Malinverno[6, 7], Gerald Langer[2], and Colin Brownlee[2, 8]

[1]BRIDGE, School of Geographical Sciences, University of Bristol, University Road, Bristol BS8 1SS, UK
[2]Marine Biological Association, The Laboratory, Citadel Hill, Plymouth PL1 2PB, UK
[3]The Lyell Centre for Earth Marine Science Technology, Heriot-Watt University, Edinburgh, UK
[4]Division for Marine and Environmental Research, Ruđer Bošković Institute, Bijenička cesta 54, 10000 Zagreb, Croatia
[5]Oceanography Section, Istituto Nazionale di Oceanografia e di Geofisica Sperimentale - OGS, via Piccard 54, 34151 Trieste, Italy
[6]University of Milano-Bicocca, Department of Earth and Environmenal Sciences, Piazza della Scienza, 4 - 20126 Milano, Italy
[7]Consorzio Nazionale Interuniversitario per le Scienze del Mare - CoNISMa, Piazzale Flaminio 9 - 00196 Roma, Italy
[8]School of Ocean and Earth Science, University of Southampton, Southampton SO14 3ZH, UK

Correspondence: Joost de Vries (joost.devries@bristol.ac.uk)

Abstract. Coccolithophores are globally important marine calcifying phytoplankton that utilize a haplo-diplontic life cycle. The haplo-diplontic life cycle allows coccolithophores to divide in both life cycle phases, and has been proposed to allow coccolithophores to expand their niche space. To-date research has however largely overlooked the life cycle of coccolithophores, and has instead focused on the diploid life cycle phase. Through a synthesis of global scanning electron microscopy (SEM) coc-

5 colithophore abundance data (n = 2534), we show that the haploid life cycle phase contributes significantly to coccolithophore abundance, constituting ≈18 % of species abundance for which haploid-diploid pairs are defined. Using hypervolumes to quantify the niche space of coccolithophores, we furthermore show that the haploid and diploid life cycle phases inhabit contrasting niches, and that this allows coccolithophores to expand their niche space by ≈17 %. Our results highlight that future coccolithophore research should consider both life cycle stages, as omission of the haploid life cycle phase in current research

10 limits our understanding of coccolithophore ecology.

1 Introduction

Coccolithophores are marine phytoplankton that produce calcium carbonate platelets, called 'coccoliths', which can be seen from space when coccolithophores bloom. Coccoliths eventually rain down into the ocean interior or serve as ballasts as they are incorporated into faecal pellets and aggregates, which drives the carbonate pump and increases organic carbon export rates

15 to the deep sea (Klaas and Archer, 2002). Through the production of coccoliths, coccolithophores produce ≈1.5 Pg of inorganic carbon per year (Hopkins and Balch, 2018; Krumhardt et al., 2019), and subsequently account for 30 % to 90 % of carbonate in sediments (Broecker and Clark, 2009).

In addition to the carbonate pump, coccolithophores contribute to the organic carbon pump, accounting for 1-40 % of marine primary production depending on habitat (Poulton et al., 2007, 2013). Because of involvement in the ocean carbon pumps and food web, coccolithophores thus play an important role in the ocean on regional to global spatial scales and seasonal to geological time scales.

Much focus has been put on understanding coccolithophore ecology and physiology, such as the function of calcification (Young, 1994; Monteiro et al., 2016; Xu et al., 2016), their diversity (Aubry, 2009; Young et al., 2003), the factors controlling their calcification (Zondervan, 2007; Taylor et al., 2017) and competitiveness (Margalef, 1978; Krumhardt et al., 2017). However, one factor that significantly impacts coccolithophore calcite production and potentially their global success, has been given little attention: their distinctive life cycle.

The life cycle of an organism is defined by the number of chromosome sets (the 'ploidy level') of the cell when asexual reproduction ('mitosis') occurs. If mitosis occurs when the cell has one set of chromosomes (a haploid cell) the life cycle is called 'haplontic' (Fig. 1a), while if mitosis occurs when the cell has two sets of chromosomes (a diploid cell) the life cycle is called 'diplontic' (Fig. 1b). A few organism can divide in both the haploid and diploid phase. Such a life cycle is called 'haplo-diplontic' (Fig. 1c). Coccolithophores utilize the latter life cycle strategy - which is in contrast to dinoflagellates and diatoms which tend to be either haplontic or diplontic, and as such can only divide in either the haploid or diploid life cycle phase (Von Dassow and Montresor, 2011).

The haploid and diploid life cycle phases of coccolithophores can vary significantly in terms of coccolith structure, size and morphology, cell size, and degree of calcification (Fig. 2). The diploid life cycle phases tend to be more heavily calcified than the haploid life cycle phases, which tend to be more lightly, or non-calcified (Cros et al., 2000; Daniels et al., 2016; Fiorini et al., 2011a, b). This difference in cell calcium carbonate content, cell organic carbon content, and ratio thereof (the PIC:POC ratio), between the two life cycle phases means that the two phases potentially have contrasting impacts on the carbonate pump.

Although coccolithophore morphology is highly diverse, the diploid phases of coccolithophores primarily utilize heterococcolithophore morphology (with some exceptions, i.e. *Braarudosphaera bigelowii*), while the haploid life cycle phases can broadly be classified into four morphologies: polycrater (Fig. 2a), ceratolith (Fig. 2b), holococcolith (Fig. 2c-i) and unmineralized (not pictured) (Frada et al., 2018). Of these four haploid morphologies, the holococcolithophore morphology - which is defined by rhomboid calcite structures that constitute the coccoliths - is the most frequent utilized (Frada et al., 2018). Eight coccolithophore clades utilize holococcoliths, while four clades utilize an unmineralized haploid morphology, one clade utilizes a ceratolith morphology, one clade utilizes ceratolith morphology, and for five clades the haploid morphology is currently unknown (Frada et al., 2018).

Coccolith and coccosphere morphology, cell and coccosphere size, and the degree of calcification influences coccolithophore ecology (Young, 1994). We can thus expect that the haploid and diploid life cycle phases of coccolithophores can have contrasting ecological preferences, which has been proposed to allow a coccolithophore species to occupy multiple niches (Houdan et al., 2006; Frada et al., 2012; Cros and Estrada, 2013; Godrijan et al., 2018; Frada et al., 2018). This ability to occupy multiple niches should expand the total niche space coccolithophore can inhabit, a potential advantage for haplo-diplontic organisms in

variable environments (Mable and Otto, 1998). An idea which is supported by genetic models (Hughes and Otto, 1999; Rescan et al., 2015).

While niche differentiation has been widely observed for haplo-diplontic seaweeds (Couceiro et al., 2015; Guillemin et al.,
55 2013; Lees et al., 2018; Lubchenco and Cubit, 1980), and coccolithophores (Houdan et al., 2006; Cros and Estrada, 2013; Godrijan et al., 2018; Frada et al., 2018), to-date no research has quantitatively investigated the extent of niche overlap and niche expansion for haplo-diplontic algae. For coccolithophores this is because research has primarily focused on the diploid life phases, and relatively little is known in regards to the haploid life phase (Taylor et al., 2017; Frada et al., 2018). This is in part due to a research focus on the globally ubiquitous *Emiliania huxleyi* which utilizes an unmineralized haploid morphology
60 which cannot be readily identified with conventional light or scanning electron microscopy (Frada et al., 2008).

With the aim of understanding how haploid coccolithophores contribute to coccolithophore success, we quantify the niche overlap and niche expansion between haploid and diploid life stages of coccolithophores for the first time.

To do so, we compile global coccolithophore abundance observations of coccolithophores using all available SEM measurements and where appropriate corresponding environmental measurements (temperature, salinity, fixed nitrogen, phosphate, and
65 silicate). Although our focus is on holococcolith forming clades rather than *E. huxleyi*, holococcolith forming clades include ecologically relevant species such as *Helicosphaera carteri* (Fig. 2e), *Coccolithus pelagicus* and *Calcidiscus leptoporus* (Fig. 2i) which contribute more to the $CaCO_3$ flux to the deep ocean than *E. huxelyi* due to their larger coccolith and coccosphere size (Ziveri et al., 2007; Rigual Hernández et al., 2019).

In addition to niche overlap and niche expansion, we investigate the dataset to identify ecological preferences of holococ-
70 colith forming species, providing an updated picture on their global distribution, relative abundance, niche space, and environmental controls. This work provides key information to better understand how the haplo-diplontic life cycle contributes to coccolithophore success.

2 Methods

2.1 Metadata compilation

75 Coccolithophore abundance measurements were compiled from 36 studies, constituting 2534 measurements, and representing all major oceans (Table 1). These studies utilized scanning electron microscopy (SEM) to enumerate or further identify coccolithophores rather than soley relying on the more commonly utilized light or cross polarized microscopy which under-represents coccolithophore biodiversity (Godrijan et al., 2018), in particular holococcolithophores (Bollmann et al., 2002; Cerino et al., 2017). We used this data set to investigate global, and vertical distribution patterns of haploid and diploid coccolithophore life
80 cycle phases, specifically focusing on holococcolith forming species.

In addition to the global data set, we further investigated three case studies, in order to better understand specific drivers and differences between the life cycle phases: the Atlantic Meridional Transect (AMT), representative of mid-oligotrophic open ocean ecosystems, the long term time series at Bermuda (BATS), and two times series in a mesotrophic coastal ecosystem in the Adriatic Sea (the 'Mediterranean data set'). For the AMT study, we considered observations from 4 cruises, specifically AMT-

85 12 (May-Jun 2003), AMT-14 (Apr-Jun 2004), AMT-15 (Sep-Oct 2004) and AMT-17 (Oct-Nov 2005) previously published by Poulton et al. (2017). For the BATS station we considered data published by Haidar and Thierstein (2001), which consists of approximately monthly observations between January 1991 to January 1994. For the Mediterranean study, we combine two time-series in the Adriatic Sea by Godrijan et al. (2018) and Cerino et al. (2017), between September 2008 to December 2009 and May 2011 to February 2013 at the RV-001 and C1-LTER stations respectively.

90   For the AMT and Mediterranean case studies, we additionally compiled temperature, salinity, and concentrations of fixed nitrogen (nitrite + nitrate), phosphate, and silicate. For the AMT environmental variables were acquired from the British Oceanographic Data Centre (BODC). For the Mediterranean study, day length was calculated using the MIT Skyfield package in Python.

    All data was acquired from supplementary data, online databases, or if neither was available by contacting the authors di-
95 rectly. The data was manually checked for synonyms or misspellings of species names, and where appropriate cell abundances were converted to cells l^{-1}. All species, or genera if not identified to a species level, were labeled as either heterococcolithophore, holococcolithophore, or 'other', which includes polycrater, nanoliths, and unidentified species. For these categorizations we followed definitions from Cros and Fortuño (2002).

    The species and environmental data were compiled in Python, and subsequently analysed in R (R Core Team, 2019). For
100 all analysis we only considered samples within the top 200 m of the water column. On a global scale and regional scale, we calculated the mean and highest observed abundances (the 'maximum abundance') of both hetero- and holococcolithophores. For the mean abundance calculations the mean was calculated for each sample and then averaged.

2.2   Definition of pairs and HOLP-index

Not all heterococcolithophore forming coccolithophore species form holococcospheres. Thus, to better illustrate the proportion
105 of haploid and diploid coccolithophore cells, we reported the ratio between hetero- and holococcospheres of species that form holococcoliths in their haploid phase, which is commonly implemented (Cros and Estrada, 2013; Šupraha et al., 2016).

    This ratio is referred to as the 'HOLP-index', and is defined by Cros and Estrada (2013) as:

$$\text{HOLP-index} = 100 \cdot \frac{\text{paired holococcolithophore abundance}}{\text{paired coccolithophore abundance}} \tag{1}$$

    Species included in the HOLP-index follow the definitions of paired species as defined in Frada et al. (2018) (Table 2)
110 - which is confined to currently understood associations and which is likely to change as our understanding holococcolith species continues to improve. We calculated the HOLP-index on a global and regional level for studies that identified holococcolithophores to a species level, the AMT data set, and the Mediterranean data set. To calculate the mean HOLP-index, the ratios were calculated for each sample and then averaged.

2.3   Environmental drivers

115 We quantified the environmental drivers of hetero- and holococcolithophore abundance and the HOLP-index for the AMT and Mediterranean data sets using Spearman correlations. We calculated Spearman correlations for hetero- and holococcol-

ithophores and the HOLP-index relative to temperature, salinity, depth, and concentrations of fixed nitrogen (nitrite + nitrate), phosphate, and silicate for the AMT data set. The same ordinal associations were calculated for the Mediterranean data set, but we considered day length instead of depth, because only the top 30 meters of the water column was sampled, and seasonality is

120   an important driver in this region. To focus on marine systems of coccolithophores, we only considered samples with salinities above 30 ppt. Samples missing any environmental variables were removed. Subsequently the AMT data set included a total of 45 samples, and the Mediterranean data set 100 samples. Spearman correlation was performed in R using the 'cor.test' function from the 'stats' package (R Core Team, 2019). We also visualised environmental drivers by plotting the distributions of cell concentrations and environmental parameters within the water column or within the first two axes of a Principal Component

125   Analysis (PCA), and then interpolating values using the Multilevel B-spline Approximation (MBA) algorithm described by Lee et al. (1997). Prior to conducting the PCA, samples with a Cook's Distance greater than 4 times the sample size were removed. For the visualizations, we used the same environmental parameters and samples as for the Spearman correlations, except for the AMT data set where we plotted chlorophyll instead of depth - which allowed visualization of the deep chlorophyll maximum (DCM). For the AMT data set, we plotted the abundance and environmental parameters as a function of latitude

130   and depth. While for the Mediterranean data set the variables were plotted as a function of the first two axes of a PCA which included temperature, salinity, day length, and concentrations of phosphate, fixed nitrogen, and silicate. The MBA interpolation was performed with the 'mba.surf' function from the 'MBA' R package (Finley et al., 2017), and the PCA was performed with the 'dudi' function of the 'ade4' package (Dray and Dufour, 2007). Cook's distances were calculated using the 'lm' and 'cooks.distance' functions provided in the 'stats' R package (R Core Team, 2019).

135   **2.4   Seasonality**

To investigate seasonality we compared monthly hetero- and holococcolithophore abundance data to temporal variations of temperature, salinity, day length, and concentrations of phosphate, fixed nitrogen, and silicate of the BATS and Mediterranean data sets.

2.5   Niche overlap and niche expansion

140   Distribution patterns of phytoplankton are influenced by multiple environmental drivers. These environmental drivers form a n-dimensional hyperspace within which hypervolumes can be defined based on where the phytoplankton occur. This hypervolume can be used to quantify niche space (Hutchinson, 1957) and allows comparisons between multiple phytoplankton - in this instance the two life cycle phases of coccolithophores.

Although processing hypervolumes is challenging due to their high dimensionality, methods described by Blonder et al.

145   (2014) allow hypervolume quantification and comparison (for futher discussion see Blonder (2018) and Mammola (2019)). Using this strategy we determine the niche overlap of hetero- and holococcolithophores in hyperspace using the Sørensen-Dice and Jaccard similarity metrics.

We furthermore calculate the 'niche expansion' of the haplo-diplontic life cycle strategy, which we define here as the non-overlapping region of either phase within hyperspace. In other words:

$$NE(A) = \frac{|A| - |A \cap B|}{|A \cup B|}$$

(2)

150

Where NE(A)= niche expansion of A; A = hypervolume A; B = hypervolume B; ∩ = intersection between two hypervolumes; ∪ = union between two hypervolumes

We calculated the Jaccard and Sørensen-Dice similarity metrics and niche expansion for both the Atlantic Ocean and Mediterranean Sea data set. For the Atlantic Ocean, nitrogen showed high Pearson correlation to silicate ($\rho = 0.95$, p < 0.001) and phosphate ($\rho = 0.90$, p < 0.001). We thus only considered temperature, salinity and the concentration of fixed nitrogen in this region. Although no such correlations were observed for the Mediterreanean data set, to make the niche metrics comparable in both regions, the silicate and phosphate concentration of the Mediterrean data set were also excluded. The environmental data were normalized using z-scores prior to analysis. Niche overlap and niche expansion was calculated only for species for which both life cycle phases were observed.

We used the 'hypervolume' R package (Blonder and David J. Harris, 2018) to conduct our niche overlap and niche expansion analysis. Gaussian kernel density estimation (R function 'hypervolume_gaussian') was used to construct the hypervolume, the overlap metrics were calculated with the 'hypervolume_overlap_statistics' R function, and the volume and intersection of hyper volumes were calculated using the 'get_volume' R function.

3 Results

3.1 Biogeography of coccolithophores

Within our compilation heterococcolithophores showed global distribution, while holococcolithophores were noticeably absent at the ALOHA station in Hawaii and (with some exceptions) >50° S in the Southern Ocean (Fig. 3 and Table 3).

Highest maximum abundances of heterococcolithophores were observed at high latitudes within the Arctic circle (>66° N) ($\approx$4.37 x 10^6 cells l^{-1}), and the Southern Ocean (>40° S and <65° S) ($\approx$1.64 x 10^6 cells l^{-1}). Low maximum abundances were observed in most of the subtropical and tropical waters such as the Arabian Sea ($\approx$1.11 x 10^5 cells l^{-1}), East China Sea ($\approx$2.39 x 10^5 cells l^{-1}), and East Indian Ocean ($\approx$2.27 x 10^5 cells l^{-1}).

The regions with the highest mean heterococcolithophore abundance differed from the regions where highest maximum heterococcolithophore abundance were observed. For example, the highest mean abundance was observed in the East Indian Ocean ($\approx$1.96 x 10^5 cells l^{-1}); which was higher than the mean abundance in the Southern Ocean ($\approx$8.87 x 10^4 cells l^{-1}), North Atlantic ($\approx$9.99 x 10^4 cells l^{-1}) and Arctic Circle ($\approx$5.71 x 10^4 cells l^{-1}).

Although holococcolithophores showed low abundances at at high latitude regions in the Southern Hemisphere, highest maximum holococcolithophore abundances were observed in the Arctic circle (>66° N) ($\approx$2.23 x 10^5 cells l^{-1}). High maximum abundances were additionally observed in the Mediterranean Sea ($\approx$1.38 x 10^5 cells l^{-1}). Generally low maximum abundances

were observed at tropical and subtropical basins such as the Arabian Sea ($\approx$5.63 x 10^3 cells 1^{-1}); with exception of the East

180   Indian Ocean ($\approx$3.10 x 10^4 cells 1^{-1}). Medium maximum abundances were observed in the North Atlantic Ocean ($\approx$3.00 x 10^4 cells 1^{-1}). On average the Mediterranean Sea had the highest mean holococcolithophore abundance ($\approx$6.00 x 10^3 cells 1^{-1}), followed by the East Indian Ocean ($\approx$4.40 x 10^3 cells 1^{-1}), and the Arctic Circle ($\approx$1.70 x 10^3 cells 1^{-1}). The lowest mean abundances were observed in the Southern Ocean ($\approx$4.00 cells x 10^2 1^{-1}), and Arabian Sea ($\approx$4.60 x 10^2 cells 1^{-1}).

Overall holococcolithophores contributed 7.3 % ($\pm$16 %) to total coccolithophore abundance globally, with their highest

185   contribution observed in the Mediterranean Sea (16.5 % $\pm$22.7 %) (Table 3). However, on a regional basis (Table 4) holococcolithophores generally contributed less than 6 % to total coccolithophore abundances. The contribution of holococcolithophores to paired species was much higher than when all hetero- and holococcolithophores are considered (Table 4), with a HOLP-index of 18.3 % ($\pm$28.2 %) globally, and the highest HOLP indices observed off the coast of Chile in the South Pacific (36.2 % $\pm$ 37.4 %), the Central Atlantic (30.2 % $\pm$ 25.2 %), and the Mediterranean Sea (27.7 % $\pm$ 30.1 %). The average

190   HOLP-index was above 15.7 % for all locations, except in the Southern Ocean where an HOLP-index of 7.1 % ($\pm$23.7 %) was observed.

3.2 Vertical distribution

In the global data set heterococcolithophore abundance is evenly distributed with depth, while holococcolithophore abundance is highest in the top 50 m of the water column (Fig. 4).

195   For holococcolithophores the vertical distribution pattern is mainly driven by paired holococcolithophore species which constituted $\approx$62.2 % to total coccolithophore abundance. Two currently unpaired holococcolithophores also contribute to the depth distribution trend with *Helladosphaera cornifera* (for which the association has to be further confirmed) constituting $\approx$8.1 % of total holococcolithophore abundance, and *Corisphaera gracilis* (for which no pair has been described) constituting $\approx$3.6 % of total holococcolithophore abundance. Subsequently paired holococcolithophore abundances broadly followed the

200   same patterns observed when all holococcolithophores were considered.

In comparison to holococcolithophores, depth distribution of heterococcolithophores was driven by unpaired species - in particular *E. huxleyi* which constituted $\approx$59.2 % of total heterococcolithophore abundance, but also by the presence of unpaired deep water species such as *Ophiaster formosus*, *Florisphaera profunda*, *Calciopappus caudatus*, and *Oolithotus antillarum*. However, although paired heterococcolithophores only contributed $\approx$5.7 % to total heterococcolithophore abundance, the depth

205   distribution trends of paired and total heterococcolithophores species were similar.

3.3 Environmental drivers of niche partitioning

To further understand the distribution patterns observed on a global basis and within the water column we investigated the environmental drivers of hetero- and holococcolithophore abundance in the Atlantic Ocean (with the AMT data set) and the Mediterranean Sea. For the Atlantic Ocean data set, the environmental drivers were considered in the context of their distri-

210   bution within the water column, whereas for the Mediterranean the environmental drivers were considered within PCA 'niche space'. These observed patterns were then further corroborated through Spearman analysis.

3.3.1 Atlantic Ocean

In the Atlantic Ocean both hetero- and holococcolithophores have highest abundances in the top 50 m of the water column (Fig. 5). However, a noticeable difference between hetero- and holococcolithophore distribution (Fig. 5a and Fig. 5d respectively)

215   is the absence of holococcolithophores below the deep chlorophyll maximum (DCM) (Fig. 5l). The DCM tends to occur at 1-10 % irradiance levels, and is closely linked to the nutricline and thermocline (Poulton et al., 2006). The difference in depth distribution between hetero- and holococcolithophores, and the absence of holococcolithophores below the DCM may therefore be influenced by a combination of light limitation, high nutrient concentrations, and cold water temperatures at depth. This suggests that heterococcolithophores might be better adapted to exploit such conditions. Although differences in sinking rates

220   - which are conceivably higher in the more heavily calcified heterococcolithophores could also factor into the difference in depth distribution between the two life cycle phases.

The distribution of heterococcolithophores (Fig. 5a) is primarily driven by *E. huxleyi* (Fig. 5c) which constitutes ≈30 % of total heterococcolithophore abundance in the data set. When only paired heterococcolithophore species were considered (Fig. 5b) a more even distribution in subtropical and tropical regions is observed. Holococcolithophores and paired holococ-

225   colithophores showed roughly similar distribution patterns (Fig. 5d and Fig. 5e).

Within the upper water column, heterococcolithophores showed highest abundance at higher latitudes (>35° N and >30° S), which is associated with a shallow mixed layer, lower salinity, and lower temperature, as well as increasing silicate concentrations in the southern hemisphere. Holococcolithophores meanwhile showed highest abundances at both high latitudes and in the Atlantic subtropical gyres. The HOLP-index (Fig. 5f) was highest within the Atlantic subtropical gyres, with a higher

230   proportion of holococcolithophores in the Northern subtropical Gyre, which is associated with a shallower DCM relative to the Southern subtropical Gyre. This shallowing of the DCM on the AMT is however likely a seasonal signal as described by Poulton et al. (2006) and Poulton et al. (2017).

Spearman correlations (Table 6) suggests holococcolithophores are significantly ($p < 0.05$) negatively correlated to phosphate, fixed nitrogen, silicate and depth and significantly positively correlated to temperature and salinity. Paired holococ-

235   lithophore and the HOLP-index showed the same correlation trends as holococcolithophores.

On the contrary, heterococcolithophores are only significantly and negatively correlated with depth and phosphate. While for paired heterococcolithophores significant negative correlations were observed with depth and silicate.

Thus hetero- and holococcolithophore abundance in the Atlantic Ocean seems primarily driven by the depth of the DCM both in terms of vertical and latitudinal distribution. Highest abundances of both hetero- and holocococlithophores are observed

240   above the DCM, and heterococcolithophores are present below the DCM while holococcolithophores are not. In terms of latitude highest abundances of heterococcolithophores correspond to shallow DCM depth which occurs in higher latitude regions, and highest abundances of holococcolithophores occur in subtropical regions with deep DCM depths.

3.3.2 Mediterranean Sea

For the Mediterranean Sea long term time series, niche separation of hetero- and holococcolithophores within the PCA niche
245 space (Fig 6), is primarily driven by Principal Component 1 (PC1) which is positively associated with temperature and day
length and negatively associated with salinity, fixed nitrogen, silicate and phosphate (see Table 7). Heterococcolithophores
are most abundant at low PC1 values (i.e. the left quadrants of Fig. 6a) which corresponds to low temperatures and short day
lengths, and high salinity and concentrations of fixed nitrogen, silicate and phosphate. Holococcolithophores are most abundant
at high PC1 values (i.e. the right quadrants of Fig. 6b), which corresponds to high temperatures and long day lengths, and low
250 salinity and concentrations of fixed nitrogen, silicate and phosphate.

The pattern observed in the PCA niche space is also apparent in the Spearman correlations (Table 6) which indicate that het-
erococcolithophores are significantly negatively correlated to temperature, and day-length, and significantly positively corre-
lated to phosphate, fixed nitrogen, silicate and salinity. For paired heterococcolithophore species the only significant correlation
observed was a positive correlation with silicate.

255 Holococcolithophores showed an opposite pattern to heterococcolithophores, and are significantly positively correlated to
day-length and temperature, and significantly negatively correlated to salinity, fixed nitrogen, silicate and phosphate. Paired
holococcolithophores and the HOLP-index showed significant positive correlation to temperature and day length, but no signifi-
cant correlations with the other environmental variables were observed.

3.3.3 General environmental trends

260 Our statistical analysis shows that in both the Mediterranean Sea and Atlantic Ocean holococcolithophores are generally found
in low nutrient and warm environments and high light availability. However, an opposite trend was observed between the
Atlantic Ocean and Mediterranean Sea in terms of correlation to salinity, with holococcolithophores positively correlated to
salinity in the Atlantic Ocean and negatively correlated to salinity in the Mediterranean Sea. This difference in correlation to
salinity may be explained by the different drivers of salinity in both regions. In the Atlantic Ocean, low salinity occurs at high
265 latitudes, while high salinity corresponds to mid-ocean gyres due to higher evaporation in tropical and sub-tropical regions. In
contrast, at the coastal site in the Mediterranean Sea, low salinity is strictly related to direct freshwater input and associated
nutrients. As such salinity may be simply correlated to other environmental drivers, rather than be a driver itself.

Statistically significant correlations were the same when all holococcolithophores, paired holococcolithophores or the HOLP-
index was considered at both locations - however fewer significant correlations were observed for paired holococcolithophores
270 and the HOLP-index.

The trend for heterococcolithophore is less clear when comparing the two sites: an opposite trend to holococcolithophores -
e.g. high nutrients and low temperatures - is observed in the Mediterranean Sea, but not in the Atlantic Ocean where many of
the correlations were not significant and heterococolithophore were negatively correlated to phosphate. This negative correla-
tion to phosphate is potentially due to deeper sampling in the Atlantic Ocean combined with high phosphate concentrations in
275 deep and light limited waters skewing correlations, which highlights the need to consider sampling and DCM depth when com-

paring environmental correlation between studies. It may furthermore be due to the presence of mixotrophic or heterothrophic coccolithophores at depth in the Atlantic Ocean, which are not found in the shallow coastal waters of the Mediterranean Sea.

3.4 Niche overlap and niche expansion

We conducted niche similarity and niche expansion calculations on both the Atlantic Ocean and Mediterranean data sets to
280 quantify niche space in these regions. For niche overlap we considered the Jaccard overlap and Sørensen-Dice overlap metrics which range from 0 to 1, with 1 signifying complete overlap. For niche expansion we considered the relative amount each life cycle contributed to the total niche space. In the Atlantic Ocean the niche overlap of paired species was high for both the Jaccard overlap and Sørensen-Dice overlap metrics (0.84 and 0.91 respectively, Table 8). However, for individual species the overlap metrics were highly variable ranging from 0.11 - 0.74 and from 0.20 - 0.81 for the Jaccard overlap and Sørensen-Dice
285 overlap metrics respectively. The niche expansion was higher for heterococcolithophores than holococcolithophores when all paired species were considered (see Table 8), but was again highly variable for individual species. The holococcolithophore phase of *C. mediterranea*, *S. bannockii*, *H. wallichii*, and *C. leptoporus* for instance all contributed more to the total niche space than their heterococcolithophore life cycle phase.

In the Mediterranean Sea niche overlap values were smaller, and niche expansion values were larger than in the Atlantic
290 Ocean (Table 9). Niche expansion of heterococcolithophores was also higher than holococcolithophores when all paired species were considered, but like in the Atlantic Ocean species specific exceptions were observed. The holococcolithophore phase of *C. mediterranea*, *S. histrica*, *S. strigilis* and *C. leptoporus* all contributed more to the total niche space than their heterococcolithophore life cycle phase in this region. In the Mediterranean Sea the niche space of *S. molischii* is of particular note, as no overlap between the two life cycle phases was observed, and the two unique components were of similar size (0.51 and 0.49
295 for hetero- and holococcolithophores respectively).

Although quantitative interpretation of niche space is difficult since niche space will vary depending on the number of environmental axes included (Blonder et al., 2014), these results highlight that holococcolithophores contribute significantly to the niche space of coccolithophores, in some instances contributing more to total niche space than the heterococcoclithophore phase. In this context *C. pelagicus* is particularly relevant as this species contributes significantly to the global carbonate flux
300 (Ziveri et al. (2007); Rigual Hernández et al. (2019), and is one of the key calcifiers in the Arctic Ocean (Daniels et al., 2016).

These results additionally suggest that the niche expansion and difference in niche preference between the two life cycle phases is higher in the Mediterranean Sea than the Atlantic Ocean. It is however not clear if this is because the haplo-diplontic life cycle is better suited to more variable coastal environments as suggested by Godrijan et al. (2018) or due to higher temporal sampling resolution in the Mediterranean Sea data set compared to the Atlantic Ocean data set.

305 ## 3.5 Seasonality of coccolithophores

Hetero- and holococcolithophore abundance highly varies with season at both the BATS station in the Atlantic Ocean and the long-term stations in the Mediterranean sea (Fig. 7). Both locations experience a peak of heterococcolithophores in the winter, followed by a peak of holococcolithophores at the end of spring, and in early summer. In the Atlantic Ocean, the heterococcol-

ithophore are present in high abundance for a longer period of time - overlapping with the spring peak in holococcolithophore

310 abundance (Fig. 7a).

At both locations the peak of the holococcolithophore bloom occurs in the spring and summer when water temperatures rise and the day length is longest, while heterococcolithophore abundance is highest in the winter when temperature is lowest and day length shortest. The seasonality of peak hetero- and holococcolithophore abundance may furthermore correspond to seasonal changes in mixed layer depth (MLD), as both the Atlantic Ocean and Mediterranean Sea experience increased mixing

315 in the winter and higher stratification in the summer.

No clear seasonal patterns were observed for fixed nitrogen or silicate concentrations at either location. Which suggest that although hetero- and holococcolithophores abundance is correlated to nutrient concentrations on spatial scales (see Sect. 3.3), on a seasonal scale other drivers such as temperature, light availability, and mixed layer depth predominate.

It is important to note that on a species level, individual species do not exclusively follow the seasonal hetero-holococcolithophore

320 trends described above, as illustrated in detail by the original publications (Cerino et al., 2017; Godrijan et al., 2018). For instance for *Syracosphaera molischii* and *Syracosphaera pulchra* the holococcolith rather than heterococcolith phase is the dominant life cycle phase in these time series. Furthermore the holococcolithophore phases of *S. molischii*, *Syracosphaera histrica*, *Algirosphaera robusta* and *Acanthoica quattrospina* are observed in the winter - a period when total holococcolithophore abundance is lowest. Finally on a individual level, succession does not immediately follow the previous life cycle phase with several

325 months of absence observed between peak abundance for some species (Cerino et al., 2017; Godrijan et al., 2018).

This highlights that grouped hetero-holococcolithophore abundances represents a generalization that might not always represent patterns observed for individual species. These differences from generally observed patterns could be due to variations in life strategy - such as mixotrophy, motility and grazing susceptibility - independent of life cycle phase. Suggesting that functional traits different from the life cycle phase may determine the niche space these species inhabit.

330 ## 4 Discussion

Our meta-analysis shows that holococcolithophores are important contributors to coccolithophore abundance and ecology, contributing ≈7.3 % to total coccolithophore abundance. Our analysis furthermore shows that haploid cells play an important role in coccolithophore species that calcify in their haploid phase, accounting on average for ≈18.3 % of their total abundance.

Although holococcolithophore contribution to calcium carbonate production is likely small due to their lower cellular $CaCO_3$

335 content - which is an order of magnitude lower than heterococcolithophores (Daniels et al., 2016; Fiorini et al., 2011a, b) - their role in the carbonate cycle in present, past and future oceans is not to be underestimated. A shift towards a higher proportion of holococcolithophore cells, would result in lower global calcium carbonate production which would subsequently result in lower CO_2 outgassing on short time scales. Furthermore the ballasting effect of coccolithophores would be reduced if a shift towards more lightly calcified haploid cells occurred (Hoffmann et al., 2015).

340 In terms of the ecological niche space - which is the environmental range a species inhabits - hetero- and holococcolithophores observations in our meta-analysis broadly conform to the Margalef Niche Space Model, proposed by Margalef

(1978), which posits that the distribution of phytoplankton functional groups relate broadly to turbulence, light and nutrients. Within this framework, we find that hetero- and holococcolithophores occupy an intermediate functional group located between diatoms and dinoflagellates (see Fig. 8) as proposed by Houdan et al. (2006) and Frada et al. (2018). Diploid heterococcol-

345   ithophores thus favour high nutrient, and more turbulent waters, whereas haploid holococcolithophores favour low nutrient, and more stratified waters.

Although the Margalef niche space model certainly presents a simplification that is prone to exceptions both for diatoms (see Kemp and Villareal (2018)) as well as coccolithophores (The generalist *E. huxleyi* and deep water species such as *F. profunda* are clear examples), the model broadly holds in our meta-analysis.

350   This ecological-environmental distinction of hetero- and holococcolithophores is observed in coccolithophore species distribution in our analysis in terms of geographical succession, depth distribution and seasonal trends. In the Southern Ocean and Atlantic Ocean a geographical shift from holococcolithophores to heterococcolithophores is observed as latitude and turbulence and nutrients increases. While in the Atlantic Ocean as well as the global data set a vertical shift is observed with holococcolithophores absent or at low abundance in deep nutrient rich waters. Finally, in the Mediterranean Sea, a seasonal shift is

355   observed as heterococcolithophores are most abundant in well mixed nutrient rich winter months and holococcolithophore are most abundant in nutrient poor stratified summer months.

However, some exceptions occur. For instance in the AMT data set, although heterococcolithophores are more evenly distributed with depth, maximum abundance of heterococcolithophores is in surface waters, and subsequently heterococcolithophores are negatively correlated to nutrients. Nonetheless the relation to turbulence holds: heterococcolithophore abundance

360   is highest in well mixed high latitude waters and holococcolithophore abundance is highest in stratified sub-tropical regions. Finally, many species specific exceptions occur. We highlight examples on a seasonal scale in our Mediterranean data set discussion (see Sect. 3.6), but exceptions were also noted along the AMT (see discussion in Poulton et al. (2017), and in other Mediterranean studies (Šupraha et al., 2016; **?**; Skejić et al., 2018). Which means that caution should be used when considering the niche space model for individual species.

365   ## 4.1   Niche overlap and expansion

Our study showed that the niche volume of coccolithophores is larger when holococcolithophores are included in coccolithophore niche space. This tells us two things: first, studies focused solely on heterococolithophore are underestimating coccolithophore habitat and thus inaccurately represent the coccolithophore functional group in modelling and physiological studies, which means that we might be underestimating their ability to compete with other phytoplankton, as well as the range

370   of environmental conditions they can tolerate. Secondly, we are underestimating the importance of coccolithophore primary productivity and carbonate production by not including accurate assessments of their abundance or activity.

This might be of particular relevance for *E. huxleyi*, the diploid phase of which has been of particular research focus due to high abundances (approx 59.2% in our compilation). Although our meta-analysis does not include haploid abundance data of this species, we suspect, following upon our findings on the haploid/diploid paired species, that the haploid phase of *E.*

375   *huxleyi* is also ecologically relevant. Previous studies suggest that the haploid life cycle phase of *E. huxleyi* can increase its

niche space due to streamlined metabolism (Rokitta et al., 2011), and variations in response to bacterial (Mayers et al., 2016; Bramucci et al., 2018), and viral pressures (Frada et al., 2008). Although it should be noted that in some instance, morphology rather than ploidy level seems to be the primary driver for observed differences in *E. huxleyi* (Frada et al., 2017). Overall, observations in the haploid stage of *E. huxleyi* are extremely limited due to difficulty of identifying the haploid phase with
380   regular light microscopy, highlighting the need for developing new techniques to account for this potentially important life cycle stage. Further development of the COD-FISH method as described by Frada et al. (2012) in particular would be relevant in this context.

4.2   Concluding remarks

Our compilation provides insight into the distribution of hetero- and holococcolithophores, but also highlights many gaps in
385   the data distribution and our knowledge on coccolithophore ecology. There is for instance a lack of SEM observations in the Pacific Ocean (2 studies in this compilation), and there are a limited number of time series available, which are particularly valuable due to the seasonal nature of these organisms. Patchiness of data combined with the patchiness of coccolithophore blooms is a challenge in fully assessing marine ecosystem functioning, and in providing global abundance estimations. Beside limitations of in situ measurements, size, POC and PIC measurements of paired hetero- and holococcolithophore species are
390   sparse, in particularly for holococcolithophores.

Such measurements are needed for global organic carbon and carbonate production estimates, which are critical for biogeochemical estimates, including model studies. Models which could then be used to contextualize in situ observations in biogeochemical context, and which could test response to environmental pressures presented by anthropogenic CO_2 emissions. Modelling approaches could furthermore be used to investigate drivers of distribution trends difficult to acquire with in
395   situ measurements such as the role of competition with other phytoplankton and the influence of top down control on distribution trends, both of which have shown to be important drivers of coccolithophore distribution in previous studies (Monteiro et al., 2016; Nissen et al., 2018).

A pertinent environmental driver not covered in our meta-analysis due to limited data, is the influence of carbonate chemistry within the haploid-diploid niche space. As the haploid and diploid phases of coccolithophores vary in their calcification status,
400   they may thus show different responses to carbonate chemistry. A study by Triantaphyllou et al. (2018) for instance found that holococcolithophores increased abundance in low pH waters. If this holds true on a global level, and holococcolithophores inhabit lower pH waters in terms of their niche space, this would have important implication in the context of ocean acidification. In particular because meta-analysis (Ridgwell et al., 2009; Krumhardt et al., 2017) and modelling (Ridgwell et al., 2007; Krumhardt et al., 2019) suggest a shift towards lower global calcification rates in response to ocean acidification and warming.
405   It should however be noted that the response of heterococcolithophores to ocean acidification is both strain and species dependent (Langer et al., 2006, 2009; Meyer and Riebesell, 2015), and global calcification rates might be more impacted by shifts in species compositions rather than individual response (Ridgwell et al., 2009).

Finally, additional experiments on the numerical response of hetero- and holococcolithophores to various environmental drivers such as those performed on *E. huxleyi* would allow a better understanding of individual environmental pressures, and

410 will furthermore be highly valuable for future modelling approaches. In this context a better understanding of the triggers of phase transition would additionally be highly desirable, as the lack of haploid-diploid pairs of the same strain limits genomic approaches.

5 Conclusions

Our analysis shows that holococcolithophores constitute a large proportion of total coccolithophore abundance (≈18 % for
415 paired species). Our study furthermore shows that hetero- and holococcolithophores have contrasting environmental preference, and that therefore the haplo-diplontic life cycle expands the niche space coccolithophores can inhabit by ≈17 %. Although our findings are limited to holococcolith forming species, lab studies suggest similar patterns are likely to be observed for other coccolithophore species such as *E. huxleyi*, and raises the question how much the haploid phase of this species contributes to global coccolithophore abundance.
420   These results highlight the need to include haploid cells into coccolithophore studies, both in the context of environmental studies, modelling approaches, and physiological studies. We limit our understanding of these organisms by just focusing on one life cycle phase, particularly in the context of coccolithophore response to climate change, as increased stratification in a warming climate may favour the haploid life cycle of coccolithophores.

Data availability. The data from the compilation will be available on PANGAEA

425 *Author contributions.* JV, FM, GW and CB conceptualized the manuscript. AP, JG, and FC provided data for analysis. JV curated the data, performed the formal analysis and visualized the results. JV, FM, CB, AP, JG, FC, GL, and EM interpreted the results. JV and FM prepared the manuscript with contributions from all co-authors.

Competing interests. The authors declare that they have no conflict of interest

Acknowledgements. This research was supported by a NERC GW4+ DTP and the Natural Environment Research Council (NERC) [NE/L002434/1]
430 studentship to JV. It was also supported by the Natural Environment Research Council grant (NE/N011708/1) to CB, GW, FM, and FM; the European Research Council grant ERC-ADG-670390 to CB; the NERC consortium grant (NER/O/S/2001/00680) and a NERC Fellowship (NE/F015054/1) to AP; and the Croatian Ministry of Science, Education and Sports (No. 098-0982705-2731) and European Community Research Infrastructure Action under the FP7 "Capacities" Program (SYNTHESYS, Project GB-TAF-132) to JG. The Atlantic Meridional Transect is funded by the UK Natural Environment Research Council through its National Capability Long-term Single Centre Science Pro-
435 gramme, Climate Linked Atlantic Sector Science (grant number NE/R015953/1). This study contributes to the international IMBeR project

and is contribution number 349 of the AMT programme. The C1-LTER station is part of the national and international Long Term Ecological Research network (LTER-Italy, LTER-Europe, ILTER). Data for the C1-LTER station were obtained in the framework of the EU FP7 MedSeA (Mediterranean Sea Acidification in a Changing Climate) project. Environmental and nutrient data were made available through the OGS Italian National Oceanographic Data Center (NODC). This is a scientific contribution of Project MIUR - Dipartimenti di Eccellenza
440 2018-2022 to the DISAT of Milano-Bicocca. We would like to thank for the statistical clinics provided by the Institute for Statistical Science at the University of Bristol. Finally we would like to thank everyone who as contributed data to the compilation.

References

Andruleit, H.: Status of the Java upwelling area (Indian Ocean) during the oligotrophic northern hemisphere winter monsoon season as revealed by coccolithophores, Marine Micropaleontology, 64, 36–51, https://doi.org/10.1016/j.marmicro.2007.02.001, 2007.

445 Andruleit, H., Stäger, S., Rogalla, U., and Čepek, P.: Living coccolithophores in the northern Arabian Sea: Ecological tolerances and environmental control, Marine Micropaleontology, 49, 157–181, https://doi.org/10.1016/S0377-8398(03)00049-5, 2003.

Andruleit, H., Rogalla, U., and Stäger, S.: Living coccolithophores recorded during the onset of upwelling conditions off Oman in the western Arabian Sea, Journal of Nannoplankton Research, 27, 1–14, 2005.

Aubry, M. P.: A sea of Lilliputians, Palaeogeography, Palaeoclimatology, Palaeoecology, 284, 88–113, 450 https://doi.org/10.1016/j.palaeo.2009.08.020, 2009.

Balch, W.: Re-evaluation of the physiological ecology of coccolithophores, in: Coccolithophores: from molecular processes to global impact, pp. 165–190, Springer, Berlin, https://doi.org/10.1007/978-3-662-06278-4, 2004.

Baumann, K., Boeckel, B., and Čepek, M.: Spatial distribution of living coccolithophores along an east- west transect in the subtropical South Atlantic, Journal of Nannoplankton Research, 30, 9–21, http://ina.tmsoc.org/JNR/online/30/Baumannetal2008JNR30-1.pdf, 2008.

455 Blonder, B.: Hypervolume concepts in niche- and trait-based ecology, Ecography, 41, 1441–1455, https://doi.org/10.1111/ecog.03187, 2018.

Blonder, B. and David J. Harris: hypervolume: High Dimensional Geometry and Set Operations Using Kernel Density Estimation, Support Vector Machines, and Convex Hulls, https://cran.r-project.org/package=hypervolume, 2018.

Blonder, B., Lamanna, C., Violle, C., and Enquist, B. J.: The n-dimensional hypervolume, Global Ecology and Biogeography, 23, 595–609, https://doi.org/10.1111/geb.12146, 2014.

460 Boeckel, B. and Baumann, K. H.: Vertical and lateral variations in coccolithophore community structure across the subtropical frontal zone in the South Atlantic Ocean, Marine Micropaleontology, 67, 255–273, https://doi.org/10.1016/j.marmicro.2008.01.014, 2008.

Bollmann, J., Cortés, M. Y., Haidar, A. T., Brabec, B., Close, A., Hofmann, R., Palma, S., Tupas, L., and Thierstein, H. R.: Techniques for quantitative analyses of calcareous marine phytoplankton, Marine Micropaleontology, 44, 163–185, https://doi.org/10.1016/S0377-8398(01)00040-8, 2002.

465 Bramucci, A. R., Labeeuw, L., Orata, F. D., Ryan, E. M., Malmstrom, R. R., and Case, R. J.: The Bacterial Symbiont Phaeobacter inhibens Shapes the Life History of Its Algal Host Emiliania huxleyi, Frontiers in Marine Science, 5, 1–12, https://doi.org/10.3389/fmars.2018.00188, https://www.frontiersin.org/article/10.3389/fmars.2018.00188/full, 2018.

Broecker, W. and Clark, E.: Ratio of coccolith CaCO3 to foraminifera CaCO3 in late Holocene deep sea sediments, Paleoceanography, 24, 1–11, https://doi.org/10.1029/2009PA001731, 2009.

470 Cepek, M.: Zeitliche und räumliche Variationen von Coccolithophoriden-Gemeinschaften im subtropischen Ost-Atlantik: Untersuchungen an Plankton, Sinkstoffen und Sedimenten, Ph.D. thesis, 1996.

Cerino, F., Malinverno, E., Fornasaro, D., Kralj, M., and Cabrini, M.: Coccolithophore diversity and dynamics at a coastal site in the Gulf of Trieste (northern Adriatic Sea), Estuarine, Coastal and Shelf Science, 196, 331–345, https://doi.org/10.1016/j.ecss.2017.07.013, 2017.

Charalampopoulou, A., Poulton, A. J., Tyrrell, T., and Lucas, M. I.: Irradiance and pH affect coccolithophore community composition on a 475 transect between the North Sea and the Arctic Ocean, Marine Ecology Progress Series, 431, 25–43, https://doi.org/10.3354/meps09140, 2011.

Charalampopoulou, A., Poulton, A. J., Bakker, D. C., Lucas, M. I., Stinchcombe, M. C., and Tyrrell, T.: Environmental drivers of coccolithophore abundance and calcification across Drake Passage (Southern Ocean), Biogeosciences, 13, 5917–5935, https://doi.org/10.5194/bg-13-5917-2016, 2016.

480 Couceiro, L., Le Gac, M., Hunsperger, H. M., Mauger, S., Destombe, C., Cock, J. M., Ahmed, S., Coelho, S. M., Valero, M., and Peters, A. F.: Evolution and maintenance of haploid-diploid life cycles in natural populations: The case of the marine brown alga Ectocarpus, Evolution, 69, 1808–1822, https://doi.org/10.1111/evo.12702, 2015.

Cros, L. and Estrada, M.: Holo-heterococcolithophore life cycles: Ecological implications, Marine Ecology Progress Series, 492, 57–68, https://doi.org/10.3354/meps10473, 2013.

485 Cros, L. and Fortuño, J. M.: Atlas of Northwestern Mediterranean Coccolithophores, Scientia Marina, 66, 1–182, https://doi.org/10.3989/scimar.2002.66s11, 2002.

Cros, L., Kleijne, A., Zeltner, A., Billard, C., and Young, J. R.: New examples of holococcolith-heterococcolith combination coccospheres and their implications for coccolithophorid biology, Marine Micropaleontology, 39, 1–34, https://doi.org/10.1016/S0377-8398(00)00010-4, 2000.

490 D'Amario, B., Ziveri, P., Grelaud, M., Oviedo, A., and Kralj, M.: Coccolithophore haploid and diploid distribution patterns in the Mediterranean Sea: Can a haplo-diploid life cycle be advantageous under climate change?, Journal of Plankton Research, 39, 781–794, https://doi.org/10.1093/plankt/fbx044, 2017.

Daniels, C. J., Poulton, A. J., Young, J. R., Esposito, M., Humphreys, M. P., Ribas-Ribas, M., Tynan, E., and Tyrrell, T.: Species-specific calcite production reveals Coccolithus pelagicus as the key calcifier in the Arctic Ocean, Marine Ecology Progress Series, 555, 29–47, 495 https://doi.org/10.3354/meps11820, 2016.

Dimiza, M., Triantaphyllou, M., and Dermitzakis, M.: Vertical distribution and ecology of living coccolithophores in the marine ecosystems of Andros Island (Middle Aegean Sea) during late summer 2001, Hellenic Journal of Geosciences, 43, 7–20, https://doi.org/10.1088/0004-637X/767/1/52, 2008.

Dimiza, M. D., Triantaphyllou, M. V., Malinverno, E., Psarra, S., Karatsolis, B.-T., Mara, P., Lagaria, A., and Gogou, A.: The composition 500 and distribution of living coccolithophores in the Aegean Sea (NE Mediterranean), Micropaleontology, 61, 521–540, 2015.

Dray, S. and Dufour, A. B.: The ade4 package: Implementing the duality diagram for ecologists, Journal of Statistical Software, 22, 1–20, https://doi.org/10.18637/jss.v022.i04, 2007.

Eynaud, F., Giraudeau, J., Pichon, J. J., and Pudsey, C. J.: Sea-surface distribution of coccolithophores, diatoms, silicoflagellates and dinoflagellates in the South Atlantic Ocean during the late austral summer 1995, Deep-Sea Research Part I: Oceanographic Research Papers, 46, 505 451–482, https://doi.org/10.1016/S0967-0637(98)00079-X, 1999.

Finley, A., Banerjee, S., and Hjelle, Ø.: MBA: Multilevel B-Spline Approximation, https://cran.r-project.org/package=MBA, 2017.

Fiorini, S., Middelburg, J. J., and Gattuso, J. P.: Testing the effects of elevated pCO2 on coccolithophores (prymnesiophyceae): Comparison between haploid and diploid life stages, Journal of Phycology, 47, 1281–1291, https://doi.org/10.1111/j.1529-8817.2011.01080.x, 2011a.

Fiorini, S., Middelburg, J. J., and Gattuso, J. P.: Effects of elevated CO2 partial pressure and temperature on the coccolithophore Syracosphaera 510 pulchra, Aquatic Microbial Ecology, 64, 221–232, https://doi.org/10.3354/ame01520, 2011b.

Frada, M., Probert, I., Allen, M. J., Wilson, W. H., and Vargas, C. D.: The "Cheshire Cat" escape strategy of the coccolithophore Emiliania huxleyi in response to viral infection, PNAS, 105, 15 944–15 949, https://doi.org/10.1073/pnas.0807707105, 2008.

Frada, M. J., Bidle, K. D., Probert, I., and de Vargas, C.: In situ survey of life cycle phases of the coccolithophore Emiliania huxleyi (Haptophyta), Environmental Microbiology, 14, 1558–1569, https://doi.org/10.1111/j.1462-2920.2012.02745.x, 2012.

515   Frada, M. J., Rosenwasser, S., Ben-Dor, S., Shemi, A., Sabanay, H., and Vardi, A.: Morphological switch to a resistant sub-
        population in response to viral infection in the bloom-forming coccolithophore Emiliania huxleyi, PLoS Pathogens, 13, 1–17,
        https://doi.org/10.1371/journal.ppat.1006775, 2017.

Frada, M. J., Bendif, E. M., Keuter, S., and Probert, I.: The private life of coccolithophores, pp. 1–20, https://doi.org/10.1127/pip/2018/0083,
        2018.

520   Geisen, M., Billard, C., Broerse, A. T., Cros, L., Probert, I., and Young, J. R.: Life-cycle associations involving pairs
        of holococcolithophorid species: Intraspecific variation or cryptic speciation?, European Journal of Phycology, 37, 531–550,
        https://doi.org/10.1017/S0967026202003852, 2002.

Giraudeau, J., Hulot, V., Hanquiez, V., Devaux, L., Howa, H., and Garlan, T.: A survey of the summer coccolithophore community in the
        western Barents Sea, Journal of Marine Systems, 158, 93–105, https://doi.org/10.1016/j.jmarsys.2016.02.012, http://dx.doi.org/10.1016/j.
525   jmarsys.2016.02.012, 2016.

Godrijan, J., Young, J. R., Marić Pfannkuchen, D., Precali, R., and Pfannkuchen, M.: Coastal zones as important habitats of coc-
        colithophores: A study of species diversity, succession, and life-cycle phases, Limnology and Oceanography, 63, 1692–1710,
        https://doi.org/10.1002/lno.10801, 2018.

Guerreiro, C., Oliveira, A., De Stigter, H., Cachão, M., Sá, C., Borges, C., Cros, L., Santos, A., Fortuño, J. M., and Rodrigues, A.: Late
530   winter coccolithophore bloom off central Portugal in response to river discharge and upwelling, Continental Shelf Research, 59, 65–83,
        https://doi.org/10.1016/j.csr.2013.04.016, 2013.

Guillemin, M. L., Sepúlveda, R. D., Correa, J. A., and Destombe, C.: Differential ecological responses to environmental stress in
        the life history phases of the isomorphic red alga Gracilaria chilensis (Rhodophyta), Journal of Applied Phycology, 25, 215–224,
        https://doi.org/10.1007/s10811-012-9855-8, 2013.

535   Guptha, M. V., Mohan, R., and Muralinath, A. S.: Living coccolithophorids from the Arabian Sea, Rivista Italiana di Paleontologia e Strati-
        grafia, 100, 551–573, 1995.

Haidar, A. T. and Thierstein, H. R.: Coccolithophore dynamics off Bermuda (N. Atlantic), Deep-Sea Research Part II: Topical Studies in
        Oceanography, 48, 1925–1956, https://doi.org/10.1016/S0967-0645(00)00169-7, 2001.

Hoffmann, R., Kirchlechner, C., Langer, G., Wochnik, A. S., Griesshaber, E., Schmahl, W. W., and Scheu, C.: Insight into Emiliania huxleyi
540   coccospheres by focused ion beam sectioning, Biogeosciences, 12, 825–834, https://doi.org/10.5194/bg-12-825-2015, 2015.

Hopkins, J. and Balch, W. M.: A New Approach to Estimating Coccolithophore Calcification Rates From Space, Journal of Geophysical
        Research: Biogeosciences, 123, 1447–1459, https://doi.org/10.1002/2017JG004235, 2018.

Houdan, A., Probert, I., Zatylny, C., Véron, B., and Billard, C.: Ecology of oceanic coccolithophores. I. Nutritional preferences of
        the two stages in the life cycle of Coccolithus braarudii and Calcidiscus leptoporus, Aquatic Microbial Ecology, 44, 291–301,
545   https://doi.org/10.3354/ame044291, 2006.

Hughes, J. S. and Otto, S. P.: Ecology and the Evolution of Biphasic Life Cycles, The American Naturalist, 154, 306–320,
        https://doi.org/10.1086/303241, 1999.

Hutchinson, G. E.: Concluding Remarks, in: Cold SpringHarbor Symposia on Quantitative Biology, pp. 415–427,
        https://doi.org/10.1201/9781315366746, 1957.

550   Karatsolis, B. T., Triantaphyllou, M. V., Dimiza, M. D., Malinverno, E., Lagaria, A., Mara, P., Archontikis, O., and Psarra, S.: Coccolithophore
        assemblage response to Black Sea Water inflow into the North Aegean Sea (NE Mediterranean), Continental Shelf Research, 149, 138–
        150, https://doi.org/10.1016/j.csr.2016.12.005, http://dx.doi.org/10.1016/j.csr.2016.12.005, 2017.

Kemp, A. E. and Villareal, T. A.: The case of the diatoms and the muddled mandalas: Time to recognize diatom adaptations to stratified waters, Progress in Oceanography, 167, 138–149, https://doi.org/10.1016/j.pocean.2018.08.002, 2018.

555 Kinkel, H., Baumann, K. H., and Cepek, M.: Coccolithophores in the equatorial Atlantic Ocean: Response to seasonal and Late Quaternary surface water variability, Marine Micropaleontology, 39, 87–112, https://doi.org/10.1016/S0377-8398(00)00016-5, 2000.

Klaas, C. and Archer, D. E.: Association of sinking organic matter with various types of mineral ballast in the deep sea: Implications for the rain ratio, Global Biogeochemical Cycles, 16, 63–1–63–14, https://doi.org/10.1029/2001gb001765, 2002.

Krumhardt, K. M., Lovenduski, N. S., Iglesias-Rodriguez, M. D., and Kleypas, J. A.: Coccolithophore growth and calcification in a changing

560 ocean, Progress in Oceanography, 159, 276–295, https://doi.org/10.1016/j.pocean.2017.10.007, 2017.

Krumhardt, K. M., Lovenduski, N. S., Long, M. C., Levy, M., Lindsay, K., Moore, J. K., and Nissen, C.: Coccolithophore Growth and Calcification in an Acidified Ocean: Insights From Community Earth System Model Simulations, Journal of Advances in Modeling Earth Systems, pp. 1418–1437, https://doi.org/10.1029/2018MS001483, 2019.

Langer, G., Geisen, M., Baumann, K. H., Kläs, J., Riebesell, U., Thoms, S., and Young, J. R.: Species-specific responses of calcifying algae

565 to changing seawater carbonate chemistry, Geochemistry, Geophysics, Geosystems, 7, https://doi.org/10.1029/2005GC001227, 2006.

Langer, G., Nehrke, G., Probert, I., Ly, J., and Ziveri, P.: Strain-specific responses of Emiliania huxleyi to changing seawater carbonate chemistry, Biogeosciences, 6, 2637–2646, https://doi.org/10.5194/bg-6-2637-2009, 2009.

Lee, S., Wolberg, G., and Shin, S. Y.: Scattered data interpolation with multilevel b-splines, IEEE Transactions on Visualization and Computer Graphics, 3, 228–244, https://doi.org/10.1109/2945.620490, 1997.

570 Lees, L. E., Krueger-Hadfield, S. A., Clark, A. J., Duermit, E. A., Sotka, E. E., and Murren, C. J.: Nonnative Gracilaria vermiculophylla tetrasporophytes are more difficult to debranch and are less nutritious than gametophytes, Journal of Phycology, 54, 471–482, https://doi.org/10.1111/jpy.12746, 2018.

Luan, Q., Liu, S., Zhou, F., and Wang, J.: Living coccolithophore assemblages in the Yellow and East China Seas in response to physical processes during fall 2013, Marine Micropaleontology, 123, 29–40, https://doi.org/10.1016/j.marmicro.2015.12.004, http://dx.doi.org/10.

575 1016/j.marmicro.2015.12.004, 2016.

Lubchenco, J. and Cubit, J.: Heteromorphic Life Histories of Certain Marine Algae as Adaptations to Variations in Herbivory, Ecology, 61, 676–687, https://doi.org/10.2307/1937433, 1980.

Mable, B. K. and Otto, S. P.: The evolution of life cycles with haploid and diploid phases, BioEssays, 20, 453–462, https://doi.org/10.1002/(SICI)1521-1878(199806)20:6<453::AID-BIES3>3.0.CO;2-N, 1998.

580 Malinverno, E.: Coccolithophorid distribution in the Ionian Sea and its relationship to eastern Mediterranean circulation during late fall to early winter 1997, Journal of Geophysical Research, 108, 8115, https://doi.org/10.1029/2002JC001346, http://doi.wiley.com/10.1029/2002JC001346, 2003.

Malinverno, E., Triantaphyllou, M. V., and Dimiza, M. D.: Coccolithophore assemblage distribution along a temperate to polar gradient in the West Pacific sector of the Southern Ocean (January 2005), Micropaleontology,

585 61, 489–506, https://doi.org/10.1007/BF01874407, https://www.researchgate.net/profile/Elisa{_}Malinverno/publication/298489041{_}Coccolithophore{_}assemblage{_}distribution{_}along{_}a{_}temperate{_}to{_}polar{_}gradient{_}in{_}the{_}West{_}Pacific{_}links/56e9abc608ae25ede830b17f.pdf{%}0Ahttp, 2015.

Mammola, S.: Assessing similarity of n-dimensional hypervolumes: Which metric to use?, Journal of Biogeography, 46, 2012–2023, https://doi.org/10.1111/jbi.13618, 2019.

590   Margalef, R.: Life-forms of phytoplankton as survival alternatives in an unstable environment, Oceanologica Acta, 1, 493–509, https://doi.org/10.1007/BF00202661, 1978.

Mayers, T. J., Bramucci, A. R., Yakimovich, K. M., and Case, R. J.: A bacterial pathogen displaying temperature-enhanced virulence of the microalga Emiliania huxleyi, Frontiers in Microbiology, 7, 1–15, https://doi.org/10.3389/fmicb.2016.00892, 2016.

Meyer, J. and Riebesell, U.: Reviews and syntheses: Responses of coccolithophores to ocean acidification: A meta-analysis, Biogeosciences, 595   12, 1671–1682, https://doi.org/10.5194/bg-12-1671-2015, 2015.

Monteiro, F. M., Bach, L. T., Brownlee, C., Bown, P., Rickaby, R. E., Poulton, A. J., Tyrrell, T., Beaufort, L., Dutkiewicz, S., Gibbs, S., Gutowska, M. A., Lee, R., Riebesell, U., Young, J., and Ridgwell, A.: Why marine phytoplankton calcify, Science Advances, 2, https://doi.org/10.1126/sciadv.1501822, 2016.

Nissen, C., Vogt, M., Münnich, M., Gruber, N., Haumann, F. A., Haumann, A., and Gruber, N.: Factors controlling coccolithophore biogeog-
600   raphy in the Southern Ocean, Biogeosciences Discussions, 2, 1–37, https://doi.org/10.5194/bg-2018-157, 2018.

Patil, S. M., Mohan, R., Shetye, S. S., Gazi, S., Baumann, K. H., and Jafar, S.: Biogeographic distribution of extant Coccolithophores in the Indian sector of the Southern Ocean, Marine Micropaleontology, 137, 16–30, https://doi.org/10.1016/j.marmicro.2017.08.002, http://dx.doi.org/10.1016/j.marmicro.2017.08.002, 2017.

Poulton, A. J., Holligan, P. M., Hickman, A., Kim, Y. N., Adey, T. R., Stinchcombe, M. C., Holeton, C., Root, S., and Woodward, E. M. S.:
605   Phytoplankton carbon fixation, chlorophyll-biomass and diagnostic pigments in the Atlantic Ocean, Deep-Sea Research Part II: Topical Studies in Oceanography, 53, 1593–1610, https://doi.org/10.1016/j.dsr2.2006.05.007, 2006.

Poulton, A. J., Adey, T. R., Balch, W. M., and Holligan, P. M.: Relating coccolithophore calcification rates to phytoplankton community dynamics: Regional differences and implications for carbon export, Deep-Sea Research Part II: Topical Studies in Oceanography, 54, 538–557, https://doi.org/10.1016/j.dsr2.2006.12.003, 2007.

610   Poulton, A. J., Painter, S. C., Young, J. R., Bates, N. R., Bowler, B., Drapeau, D., Lyczsckowski, E., and Balch, W. M.: The 2008 Emiliania huxleyi bloom along the Patagonian Shelf: Ecology, biogeochemistry, and cellular calcification, Global Biogeochemical Cycles, 27, 1023–1033, https://doi.org/10.1002/2013GB004641, 2013.

Poulton, A. J., Holligan, P. M., Charalampopoulou, A., and Adey, T. R.: Coccolithophore ecology in the tropical and subtropical Atlantic Ocean: New perspectives from the Atlantic meridional transect (AMT) programme, Progress in Oceanography, 158, 150–170,
615   https://doi.org/10.1016/j.pocean.2017.01.003, https://doi.org/10.1016/j.pocean.2017.01.003, 2017.

R Core Team: R: A Language and Environment for Statistical Computing, https://www.r-project.org/, 2019.

Rescan, M., Lenormand, T., and Roze, D.: Interactions between genetic and ecological effects on the evolution of life cycles, American Naturalist, 187, 19–34, https://doi.org/10.1086/684167, 2015.

Ridgwell, A., Zondervan, I., Hargreaves, J. C., Bijma, J., and Lenton, T. M.: Assessing the potential long-term increase of oceanic fossil fuel
620   CO 2 uptake due to CO2-calcification feedback, Biogeosciences, 4, 481–492, https://doi.org/10.5194/bg-4-481-2007, 2007.

Ridgwell, a., Schmidt, D. N., Turley, C., Brownlee, C., Maldonado, M. T., Tortell, P., and Young, J. R.: From laboratory manipulations to earth system models: predicting pelagic calcification and its consequences, Biogeosciences Discussions, 6, 3455–3480, https://doi.org/10.5194/bgd-6-3455-2009, 2009.

Rigual Hernández, A. S., Trull, T. W., Nodder, S. D., Flores, J. A., Bostock, H., Abrantes, F., Eriksen, R. S., Sierro, F. J., Davies, D. M.,
625   Ballegeer, A.-M., Fuertes, M. A., and Northcote, L. C.: Coccolithophore biodiversity controls carbonate export in the Southern Ocean, Biogeosciences Discussions, pp. 1–39, https://doi.org/10.5194/bg-2019-352, 2019.

Rokitta, S. D., de Nooijer, L. J., Trimborn, S., de Vargas, C., Rost, B., and John, U.: Transcriptome analyses reveal differential gene expression patterns between the life-cycle stages of emiliania huxleyi (haptophyta) and reflect specialization to different ecological niches, Journal of Phycology, 47, 829–838, https://doi.org/10.1111/j.1529-8817.2011.01014.x, 2011.

630 Saavedra-Pellitero, M., Baumann, K. H., Flores, J. A., and Gersonde, R.: Biogeographic distribution of living coccolithophores in the pacific sector of the southern ocean, Marine Micropaleontology, 109, 1–20, https://doi.org/10.1016/j.marmicro.2014.03.003, http://dx.doi.org/10.1016/j.marmicro.2014.03.003, 2014.

Schiebel, R., Zeltner, A., Treppke, U. F., Waniek, J. J., Bollmann, J., Rixen, T., and Hemleben, C.: Distribution of diatoms, coccolithophores and planktic foraminifers along a trophic gradient during SW monsoon in the Arabian Sea, Marine Micropaleontology, 51, 345–371, 635 https://doi.org/10.1016/j.marmicro.2004.02.001, 2004.

Schiebel, R., Brupbacher, U., Schmidtko, S., Nausch, G., Waniek, J. J., and Thierstein, H. R.: Spring coccolithophore production and dispersion in the temperate eastern North Atlantic Ocean, Journal of Geophysical Research, 116, 1–12, https://doi.org/10.1029/2010JC006841, 2011.

Silver, M.: Vertigo KM0414 phytoplankton species data and biomass data: abundance and fluxes from CTDs, 2009.

640 Skejić, S., Arapov, J., Kovačević, V., Bužančić, M., Bensi, M., Giani, M., Bakrač, A., Mihanović, H., Gladan, Ž. N., Urbini, L., and Grbec, B.: Coccolithophore diversity in open waters of the middle Adriatic Sea in pre- and post-winter periods, Marine Micropaleontology, 143, 30–45, https://doi.org/10.1016/j.marmicro.2018.07.006, 2018.

Smith, H. E., Poulton, A. J., Garley, R., Hopkins, J., Lubelczyk, L. C., Drapeau, D. T., Rauschenberg, S., Twining, B. S., Bates, N. R., and Balch, W. M.: The influence of environmental variability on the biogeography of coccolithophores and diatoms in the Great Calcite Belt, 645 Biogeosciences, 14, 4905–4925, https://doi.org/10.5194/bg-14-4905-2017, 2017.

Šupraha, L., Ljubešić, Z., Mihanović, H., and Henderiks, J.: Coccolithophore life-cycle dynamics in a coastal Mediterranean ecosystem: Seasonality and species-specific patterns, Journal of Plankton Research, 38, 1178–1193, https://doi.org/10.1093/plankt/fbw061, 2016.

Takahashi, K. and Okada, H.: Environmental control on the biogeography of modern coccolithophores in the southeastern Indian Ocean offshore of Western Australia, Marine Micropaleontology, 39, 73–86, https://doi.org/10.1016/S0377-8398(00)00015-3, 2000.

650 Taylor, A. R., Brownlee, C., and Wheeler, G.: Coccolithophore Cell Biology: Chalking Up Progress, Annual Review of Marine Science, 9, 283–310, https://doi.org/10.1146/annurev-marine-122414-034032, 2017.

Triantaphyllou, M. V., Baumann, K. H., Karatsolis, B. T., Dimiza, M. D., Psarra, S., Skampa, E., Patoucheas, P., Vollmar, N. M., Koukousioura, O., Katsigera, A., Krasakopoulou, E., and Nomikou, P.: Coccolithophore community response along a natural CO2 gradient off Methana (SW Saronikos Gulf, Greece, NE Mediterranean), PLoS ONE, 13, https://doi.org/10.1371/journal.pone.0200012, 2018.

655 Von Dassow, P. and Montresor, M.: Unveiling the mysteries of phytoplankton life cycles: Patterns and opportunities behind complexity, Journal of Plankton Research, 33, 3–12, https://doi.org/10.1093/plankt/fbq137, 2011.

Xu, J., Bach, L. T., Schulz, K. G., Zhao, W., Gao, K., and Riebesell, U.: The role of coccoliths in protecting Emiliania huxleyi against stressful light and UV radiation, Biogeosciences, 13, 4637–4643, https://doi.org/10.5194/bg-13-4637-2016, 2016.

Young, J.: Functions of coccoliths, in: Coccolithophores, pp. 63–82, University Press, Cambridge, 1994.

660 Young, J. R., Bown, P. R., and Lees, J. A.: Nannotax 3 website, http://www.mikrotax.org/Nannotax3.

Young, J. R., Geisen, M., Cros, L., Kleijne, A., Sprengel, C., Probert, I., and Østergaard, J.: A guide to extant coccolithophore taxonomy, Journal of Nannoplankton Research, p. 125, 2003.

Ziveri, P., de Bernardi, B., Baumann, K. H., Stoll, H. M., and Mortyn, P. G.: Sinking of coccolith carbonate and potential contribution to organic carbon ballasting in the deep ocean, Deep-Sea Research Part II: Topical Studies in Oceanography, 54, 659–675, https://doi.org/10.1016/j.dsr2.2007.01.006, 2007.

Zondervan, I.: The effects of light, macronutrients, trace metals and CO2 on the production of calcium carbonate and organic carbon in coccolithophores-A review, Deep-Sea Research Part II: Topical Studies in Oceanography, 54, 521–537, https://doi.org/10.1016/j.dsr2.2006.12.004, 2007.

665

A. Haplontic life cycle (Dinoflagellates)
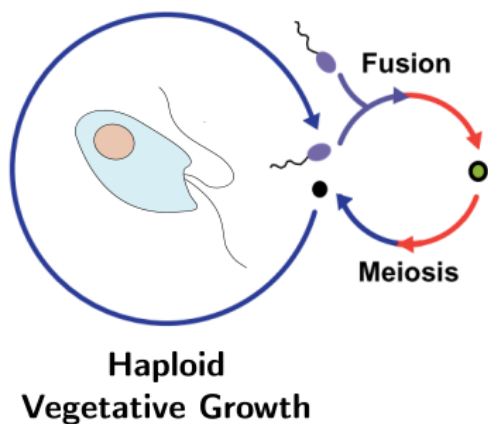
B. Diplontic life cycle (Diatoms)
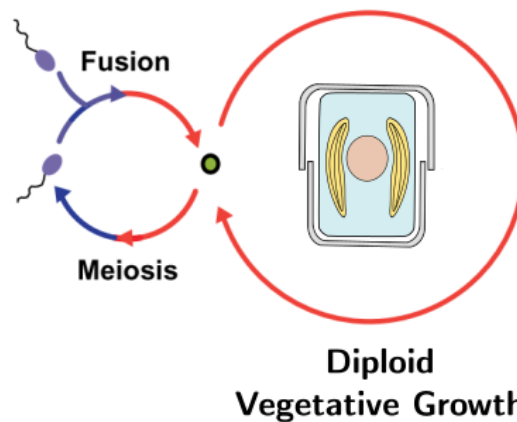
C. Haplo-diplontic life cycle (Coccolithophores)
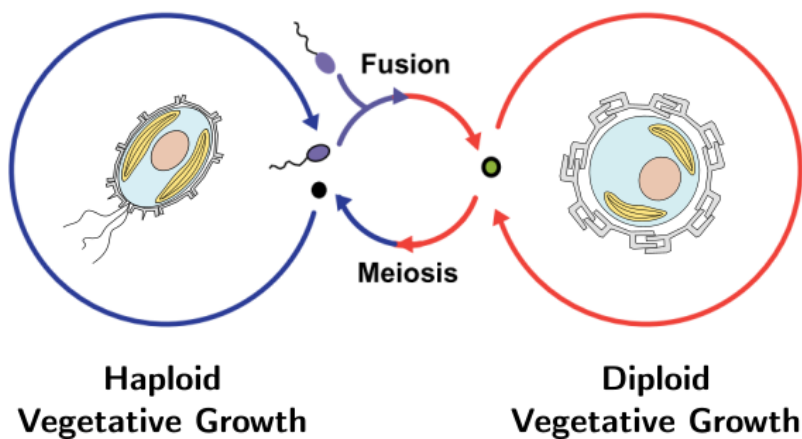
Figure 1. Life cycle strategies of phytoplankton. **(a)** Dinoflagellates tend to utilize a haplontic life cycle; **(b)** Diatoms tend to utilize a diplontic life cycle; **(c)** coccolithophores tend to utilize a haplo-diplontic life cycle. Note that not all coccolithophores calcify in their haploid phase.
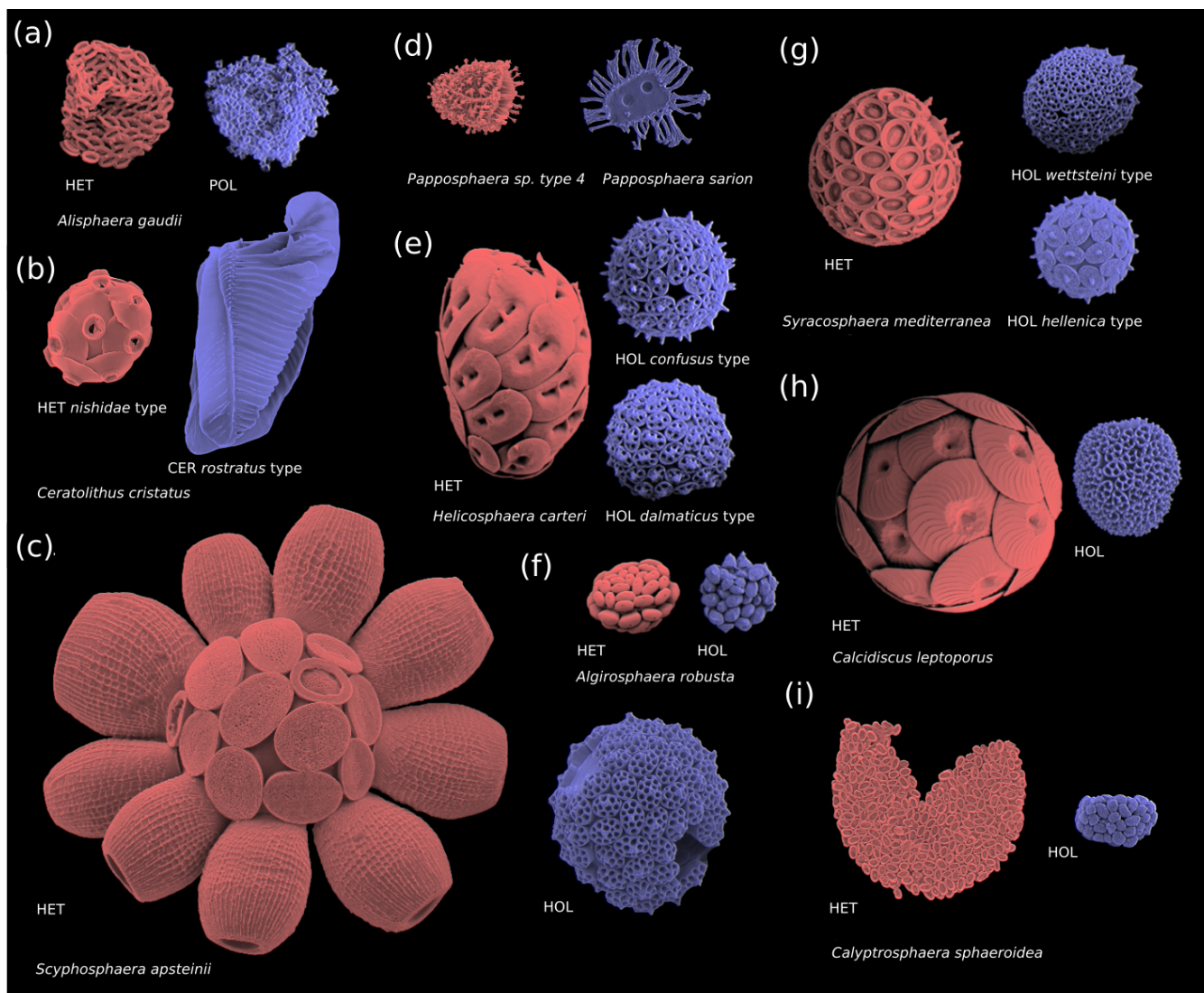
Figure 2. Coccosphere diversity of common cococcolithophores. Haploid cells are colored in blue and diploid cells in red. **(a)** Polycrater haploid morphology; **(b)** Ceratolith haploid morphology; **(c-i)**. Holococcolith haploid morphology. Note that in some instances multiple haploid phases are associated with one diploid phase (e.g. *S. mediterranea* and *H. carteri*), which may be due to cryptic speciation (Geisen et al., 2002). Furthermore, some species (e.g. *E. huxleyi*) do not calcify in their haploid phase and are thus not pictured. Images reproduced with permission from Young et al. **(b-d, i)**, and Šupraha et al. (2016) **(a, e-h)**. Images **(b-d, i (HOL))** by Jeremy Young, **(i (HET))** by Marie-Helene Kawachi, **(a, e-h)** by Luka Šupraha.
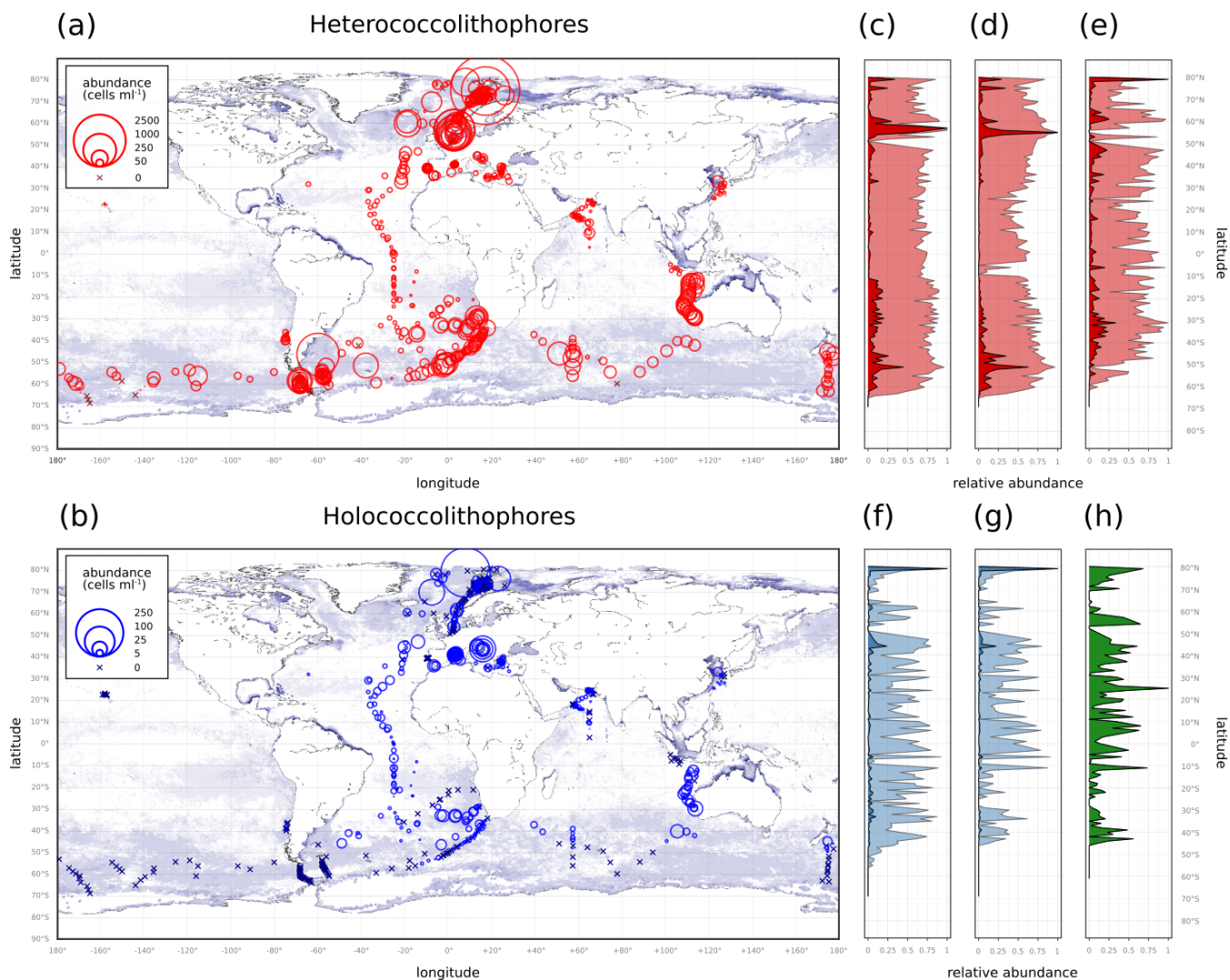
Figure 3. (a-b) Global coccolithophore distribution; **(c-h)** latitudinal coccolithophore distribution. **(a)** Heterococolithophores; **(b)** Holococ-colithophores; **(c)** Heterococcolithophores; **(d)** *E. huxleyi*; **(e)** Paired heterococolithophores; **(f)** Holococcolithophores; **(g)** Paired holococ-colithophores; **(h)** HOLP-index. For the latitudinal plots, the light shading is log transformed distribution.
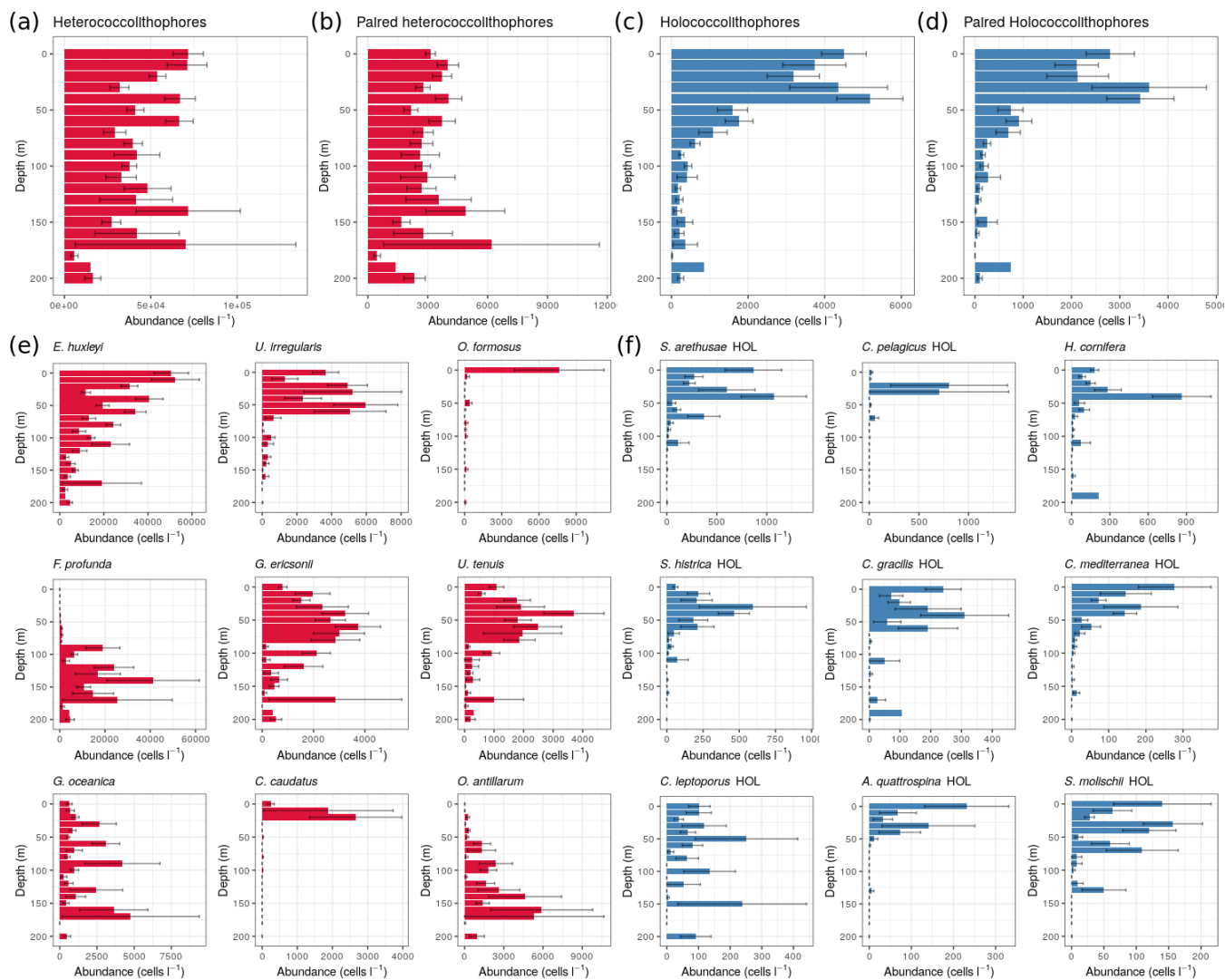
Figure 4. Global depth distribution of hetero- and holococcolithophores. **(a-d)** total paired and unpaired hetero- and holococcolithophore abundance; **(e-f)** individual species abundances. Heterococcolithophores are plotted in blue, and holococcolithophores are plotted in red. Only the most abundant coccolithophore species are plotted individually. Error bars are standard error.
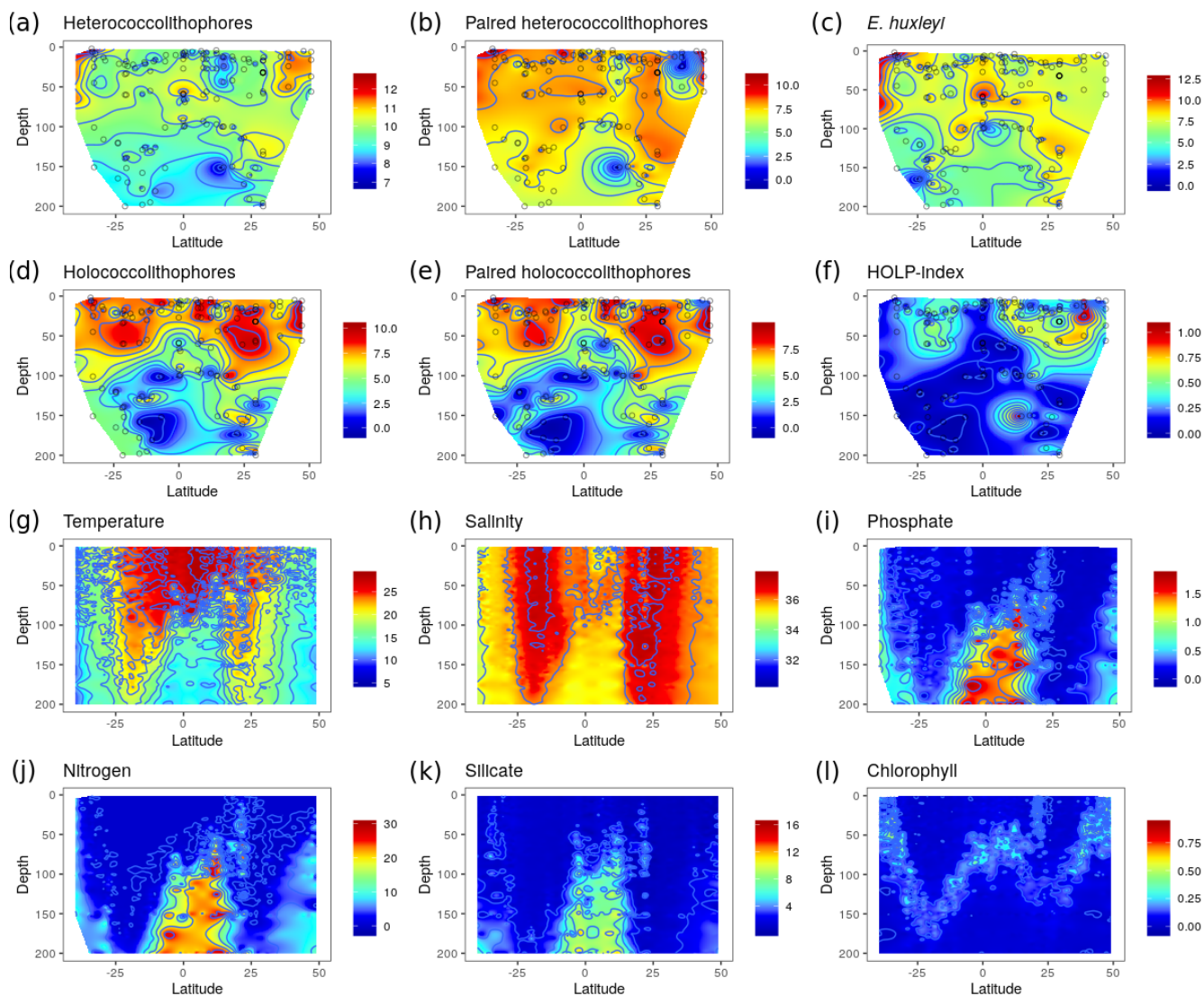
Figure 5. Depth distribution along AMT. **(a)** Heterococcolithophore abundance; **(b)** Paired heterococcolithophore abundance; **(c)** *E. huxleyi* abundance; **(d)** Holococcolithophore abundance; **(e)** Paired holococcolithophore abundance; **(f)** HOLP-index; **(g)** Temperature (° C); **(h)** Salinity (ppt); **(i)** Phosphate (μM); **(j)** Silicate (μM); **(l)** Chlorophyll. Species abundances are plotted on log scale.
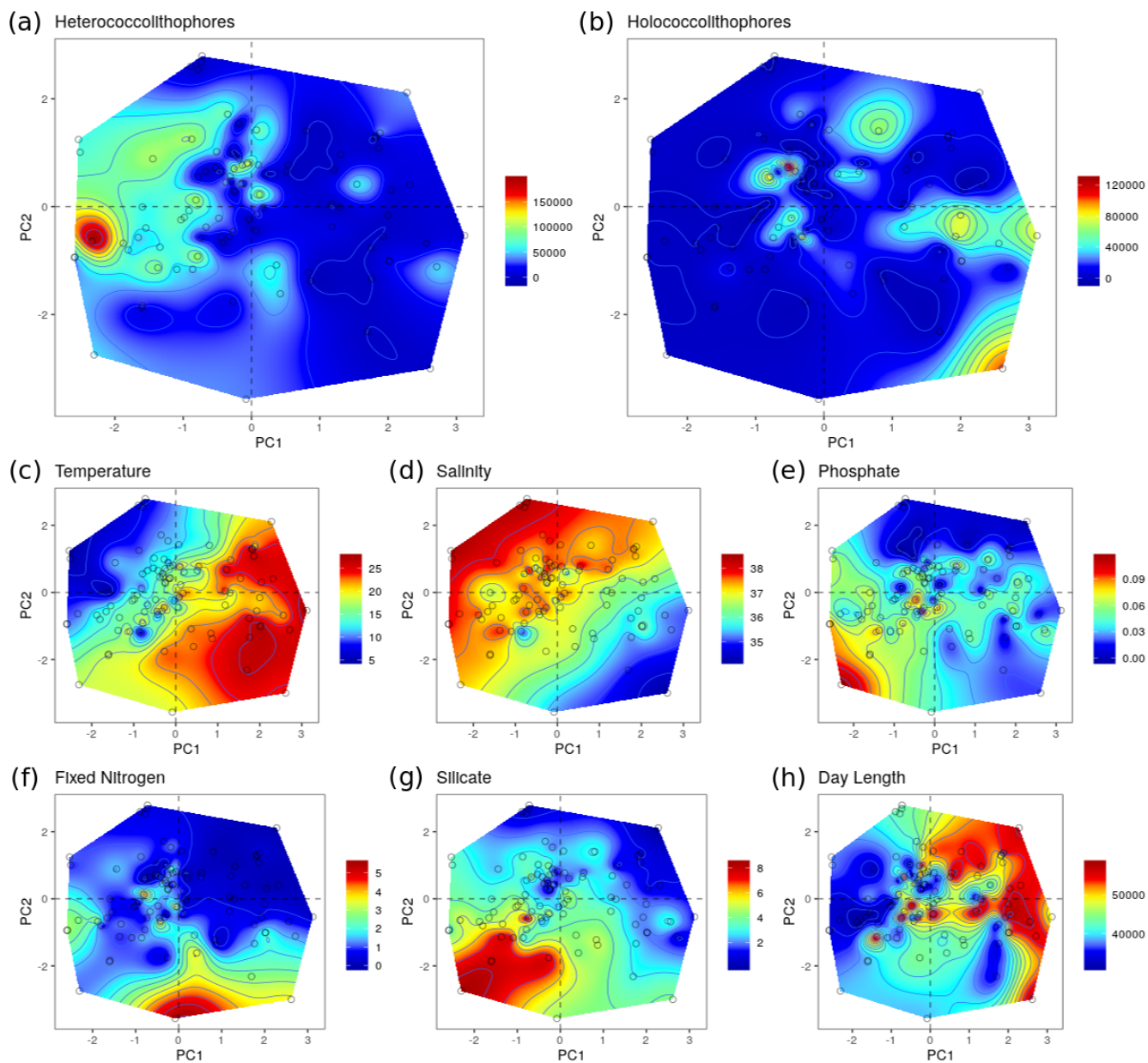
Figure 6. Principal Component analysis (PCA) of the RV-001 and LTER1 stations in the Mediterranean Sea. Abundance and environmental values were projected on the PCA *post hoc*, and then interpolated. **(a)** Heterococcolithophore abundance; **(b)** Holococcolithophore abundance; **(c)** Salinity; **(d)** Temperature; **(e)** Depth; **(f)** Phosphate; **(g)** Fixed nitrogen; **(h)** Silicate. Data was acquired from Cerino et al. (2017) and Godrijan et al. (2018).
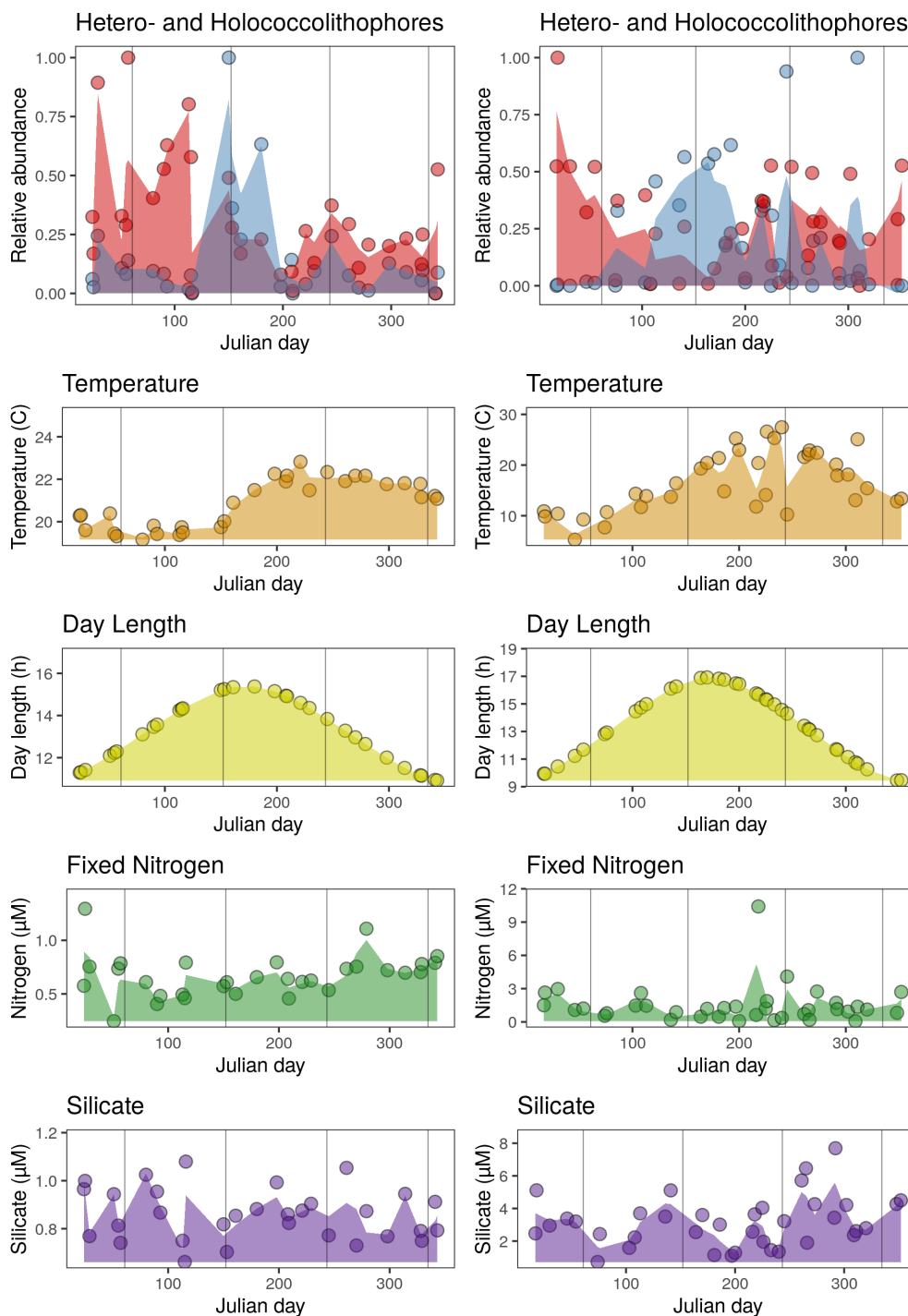
Figure 7. Seasonality of hetero- and holococcolithophores at the BATS station in Bermuda (left column) and the RV-001 and LTER-1 stations in the Mediterranean Sea (right column). For the hetero- and holococcolithophore plots, heterococcolithophores are plotted in red and holococcolithophores are plotted in blue.
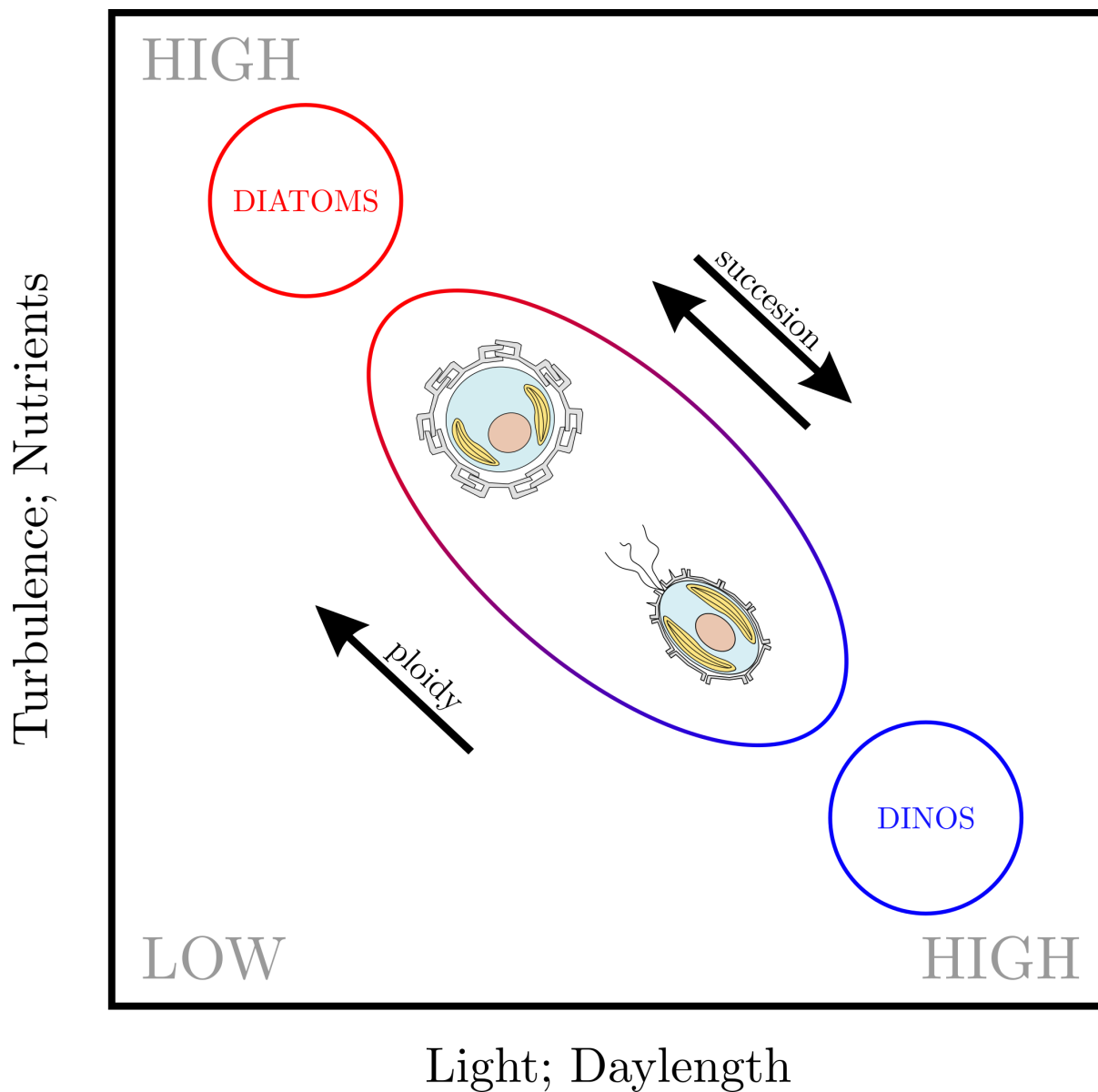
Figure 8. A. Modified version of Margalef's niche space model (Margalef, 1978) as proposed by Houdan et al. (2006) and Frada et al. (2018). Note that we have added day length, which was proposed by Balch (2004) as a third axis of the Margalef niche space model.

Table 1. Overview of Metadata.

Reference	Survey Period	Region	Method	HOLP	n
Andruleit et al. (2003)	Sep (1993)	Arabian Sea	SEM	YES	71
Andruleit et al. (2005)	Jun (2000)	Arabian Sea	SEM	NO	21
Andruleit (2007)	Jan to Feb (1999)	Indian Ocean	SEM	YES	45
Boeckel and Baumann (2008)	Mar to May (1998)	South Atlantic	SEM	YES	57
	Feb to Mar (2000)				
Baumann et al. (2008)	Feb (1993, 1996)	South Atlantic	SEM	NO	34
	Mar (1996), Dec (1999)				
Cerino et al. (2017)	Monthly (2011-2013)	Mediterranean sea	pLM/SEM	YES	84
Charalampopoulou et al. (2011)	Jul to Aug (2008)	North Sea and Arctic Ocean	SEM	YES	94
Charalampopoulou et al. (2016)	Feb to Mar (2009)	Southern Ocean	SEM	YES	103
Cepek (1996)	Feb (1993)	South Atlantic Ocean	SEM	YES	33
Cros and Estrada (2013)	Jun to Jul, and Sep (1996)	Mediterranean sea	SEM	YES	113
D'Amario et al. (2017)	Apr (2011) and May (2013)	Mediterranean sea	SEM	YES	44
Daniels et al. (2016)	Jun (2012)	Arctic Ocean	pLM/SEM	YES	19
Dimiza et al. (2008)	Apr (2002), Aug (2001 and 2002)	Mediterranean sea	SEM	YES	190
Dimiza et al. (2015)	Jan (2007), Feb (2012)	Mediterranean sea	SEM	YES	99
	Mar (2002), Apr (2006)				
	May (2013), Aug (2001)				
	Sep (2004)				
Eynaud et al. (1999)	Feb to Mar (1995)	South Atlantic Ocean	LM/SEM	NO	40
Giraudeau et al. (2016)	Aug to Sep (2014)	Barents Sea	pLM/SEM	YES	170
Godrijan et al. (2018)	Twice a month (2008-2009)	Mediterranean sea	LM/SEM	YES	24
Guerreiro et al. (2013)	Mar (2010)	Nazare Canyon, Portugal	pLM/SEM	YES	108
Guptha et al. (1995)	Sep to Oct (1992)	Arabian Sea	SEM	YES	18
Haidar and Thierstein (2001)	Jan 1991 to Jan 1994	Bermuda, North Atlantic	pLM/SEM	NO	217
Karatsolis et al. (2017)	Oct (2013), Mar (2014)	Mediterranean sea	SEM	YES	72
	Oct (2013), Jul (2014)				
Kinkel et al. (2000)	Aug to Sep (1994)	Atlantic ocean	SEM		47
	Mar to Apr (1996)				
	Jan to Mar (1997)				
Luan et al. (2016)	Oct to Nov (2013)	Yellow and East China Seas	SEM	YES	57
Malinverno (2003)	Nov to Dec (1997)	Mediterranean sea	pLM/SEM	NO	72
Malinverno et al. (2015)	Jan (2001)	Southern Ocean, West Pacific	pLM/SEM	NO	13
Patil et al. (2017)	Jan to Feb (2010)	Southern Ocean	SEM	NO	48
Poulton et al. (2017)	May to Jun (2003)	Atlantic ocean	SEM	YES	143
	Apr to Jun (2004)				
	Sep to Oct (2004)				
	Oct to Nov (2005)				
Saavedra-Pellitero et al. (2014)	Nov (2009) to Jan (2010)	Southern ocean	SEM	NO	150
Schiebel et al. (2011)	Mar (2004)	North Atlantic Ocean	SEM	NO	47
Schiebel et al. (2004)	May to Jun (1997)	Arabian Sea	SEM	YES	49
	and Jul to Aug (1995)				
Smith et al. (2017)	Jan to Feb (2011),	Southern Ocean	SEM	NO	27
	Feb to Mar (2012)				
Šupraha et al. (2016)	Feb (2013) and Jul (2013)	Mediterranean sea	SEM	YES	63
Takahashi and Okada (2000)	Feb to Mar (1996)	SE Indian Ocean	SEM	NO	118
Triantaphyllou et al. (2018)	Mar (2017)	Mediterranean sea	LM/SEM	YES	42
	Mar (2017)				
Silver (2009)	Jan (2004) to Jun (2004)	Pacific Ocean (HOT)	SEM	NO	13

Table 2. Taxanomic units included in HOLP-index

Heterococcolithophores	Holococcolithophores
C. mediterranea	*C. mediterranea* HOL
S. pulchra	*S. pulchra* HOL
S. protrudens	
S. bannockii	*S. bannockii* HOL
S. nana	*S. nana* HOL
S. arethusae	*S. arethusae* HOL
S. nodosa	*H. cornifera*
S. histrica	*S. histrica* HOL
S. molischii	*S. molischii* HOL
S. anthos	*S. anthos* HOL
S. strigilis	*S. strigilis* HOL
S. halldalii	*S. halldalii* HOL
S. marginiporata	*S. marginiporata* HOL
S. apsteinii	*S. apsteinii* HOL
P. japonica	*P. japonica* HOL
H. carteri	*H. carteri* HOL
H. wallichii	*H. wallichii* HOL
H. pavimentum	*Helicosphaera* HOL *dalmaticus* type
A. quattrospina	*A. quattrospina* HOL
A. robusta	*S. quadridentata*
R. clavigera	
R. xiphos	
C. aculeata	*C. heimdaliae*
C. leptoporus	*C. leptoporus* HOL
C. pelagicus	*C. pelagicus* HOL
C. quadriperforatus	*C. quadriperforatus* HOL
C. sphaeroidea	*C. sphaeroidea* HOL
P. arctica	*P. arctica* HOL
P. sagittifera	*P. sagittifera* HOL
P. borealis	*P. borealis* HOL
B. virgulosa	*B. virgulosa* HOL

Table 3. Global hetero- and holococcolithophore abundance

Location	spp	mean (cells L^{-1})	max (cells L^{-1})	contribution (%)	n
Global	HET	54100 (± 142353)	4365960	89.225 (±19.178)	2534
Global	HOL	2754 (±10832)	223100	7.258 (±15.959)	2534
Global	Other	2086 (±14343)	436564	3.517 (±8.942)	2534
Arabian Sea	HET	13776 (±19675)	110600	89.67 (±15.967)	159
Arabian Sea	HOL	458 (±961)	5632	5.036 (±13.681)	159
Arabian Sea	Other	775 (±2003)	17194	5.294 (±9.777)	159
Arctic Circle	HET	57140 (±328195)	4365960	93.275 (±21.523)	225
Arctic Circle	HOL	1743 (±15799)	223100	3.721 (±14.593)	225
Arctic Circle	Other	40 (±675)	7200	34 (±16.517)	225
Central Atlantic	HET	18846 (±19308)	98822	92.082 (±11.02)	164
Central Atlantic	HOL	1265 (±2609)	17588	5.83 (±9.092)	164
Central Atlantic	Other	468 (±1027)	7748	2.089 (±3.695)	164
East China Sea	HET	29796 (±47418)	238701	96.331 (±14.46)	51
East China Sea	HOL	906 (±2908)	14664	3.528 (±14.473)	51
East China Sea	Other	22 (±112)	647	0.141 (±0.785)	51
East Indian Ocean	HET	195737 (±11491)	227000	96.553 (±3.365)	118
East Indian Ocean	HOL	4441 (±6255)	31000	2.224 (±3.138)	118
East Indian Ocean	Other	2475 (±2410)	12000	1.223 (±1.203)	118
Hawaii	HET	786 (±504)	1840	89.357 (±15.303)	13
Hawaii	HOL	0 (±0)	0	0 (±0)	13
Hawaii	Other	50 (±63)	220	10.643 (±15.303)	13
Mediterranean Sea	HET	20474 (±36834)	396340	79.158 (±26.052)	756
Mediterranean Sea	HOL	6008 (±16640)	137805	16.521 (±22.696)	756
Mediterranean Sea	Other	2987 (±23043)	436564	4.322 (±8.976)	756
North Atlantic	HET	92498 (±213373)	1548984	96.414 (±6.726)	211
North Atlantic	HOL	1470 (±4486)	30051	1.712 (±4.716)	211
North Atlantic	Other	1009 (±2488)	17277	1.874 (±4.083)	211
South Pacific Ocean	HET	22009 (±33278)	159815	95.332 (±12.559)	49
South Pacific Ocean	HOL	44 (±156)	732	0.146 (±0.444)	49
South Pacific Ocean	Other	3006 (±9037)	40097	4.521 (±12.575)	49
Southern Ocean	HET	94291 (±148966)	1636130	97.918 (±8.06)	382
Southern Ocean	HOL	397 (±1983)	26668	0.997 (±6.076)	382
Southern Ocean	Other	329 (±856)	5257	1.085 (±5.414)	382

Values in parentheses are standard deviations.

Table 4. Global HOLP-index

Location	mean (%)	n
Global	18.33% (±28.19%)	1836
Arabian Sea	18% (±34.83%)	102
Arctic Circle	15.66% (±31.89%)	108
Central Atlantic	16% (±23.94%)	117
East China Sea	17.06% (±26.61%)	40
East Indian Ocean	0%	85
Hawaii	0%	9
Mediterranean Sea	27.69% (±30.08%)	709
North Atlantic	16.43% (±25.41%)	174
South Pacific Ocean	36.19% (±37.43%)	30
Southern Ocean	7.05% (±23.73%)	141

Values in parentheses are standard deviations.

Table 5. PCA loadings of Mediterranean Sea data set

Variable	PC1	PC2
Temperature	1.57	-0.75
Salinity	-1.25	1.23
Fixed Nitrogen	-0.42	-1.04
Silicate	-0.98	-1.27
Phosphate	-0.81	-0.89
DayLength	1.17	0.27

The first two axis of the PCA captured
53.94% of variance. Data from Cerino et al.
(2017) and Godrijan et al. (2018)

Table 6. Spearman correlations for AMT data set

Phase	Temp	Sal	PO4	NOx	Depth	Si
HET	-0.095	-0.085	**-0.298***	-0.095	**-0.323*****	-0.139
HET.P	0.13	0.136	-0.069	-0.092	**-0.384*****	**-0.295****
HOL	**0.339*****	**0.224****	**-0.327***	**-0.609*****	**-0.584*****	**-0.52*****
HOL.P	**0.327*****	**0.233****	**-0.289***	**-0.55*****	**-0.58*****	**-0.502*****
HOLP	**0.31*****	**0.236****	**-0.506*****	**-0.587*****	**-0.472*****	**-0.469*****

*** p<0.001, ** p<0.01, * p<0.05

Significant correlations are highlighted in bold. Data was acquired from Poulton et al. (2017).

Table 7. Spearman correlations for Mediterranean data set

Phase	Temp	Sal	PO4	NOx	DayLen	Si
HET	**-0.304****	**0.324****	**0.213***	**0.351*****	**-0.329****	**0.373*****
P.HET	0.096	0.18	0.08	-0.009	0.029	**0.208***
HOL	**0.443*****	**-0.365*****	-0.071	**-0.295****	**0.475*****	-0.155
P.HOL	**0.359*****	-0.056	0.042	-0.079	**0.357*****	0.029
HOLP	**0.418*****	-0.145	0.018	-0.063	**0.399*****	-0.031

*** p<0.001, ** p<0.01, * p<0.05

Significant correlations are highlighted in bold. Data was acquired from Godrijan et al. (2018) and Cerino et al. (2017)

Table 8. Niche expansion and niche overlap in Atlantic Ocean

Species	NE1	NE2	Jaccard	Sørensen
Paired species	0.11	0.05	0.84	0.91
S. pulchra	0.18	0.14	0.68	0.81
C. mediterranea	0.06	0.46	0.48	0.65
S. molischii	0.44	0.32	0.24	0.39
S. histrica	0.36	0.17	0.47	0.64
A. quattrospina	0.50	0.05	0.45	0.62
S. bannockii	0.17	0.19	0.63	0.77
S. nana	0.50	0.06	0.44	0.62
S. anthos	0.69	0.04	0.27	0.42
S. halldalii	0.17	0.08	0.74	0.85
H. carteri	0.41	0.30	0.29	0.45
H. wallichii	0.42	0.47	0.11	0.20
C. leptoporus	0.21	0.45	0.34	0.51

NE1 = Heterococcolithophore niche expansion,

NE2 = Holococcolithophore niche expansion

Table 9. Niche expansion and niche overlap in Mediterranean Sea

Species	NE1	NE2	Jaccard	Sørensen
Paired species	0.31	0.15	0.54	0.70
S. pulchra	0.51	0.16	0.33	0.49
C. mediterranea	0.22	0.42	0.37	0.54
S. molischii	0.47	0.53	0.00	0.00
S. histrica	0.03	0.78	0.19	0.32
A. quattrospina	0.47	0.18	0.35	0.52
S. arethusa	0.26	0.29	0.45	0.62
S. strigilis	0.12	0.53	0.35	0.52
C. leptoporus	0.26	0.61	0.13	0.23

NE1 = Heterococcolithophore niche expansion,

NE2 = Holococcolithophore niche expansion